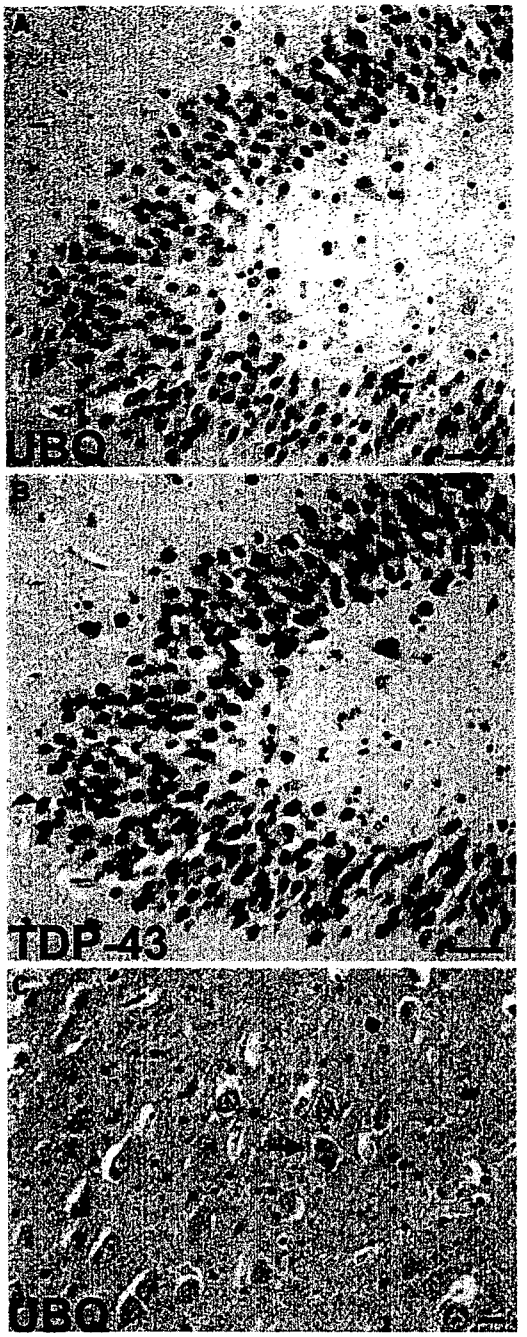

Fig. 12 Frontotemporal lobar degeneration with *CHMP2B* mutation. **a** Sparse ubiquitin-immunoreactive NCIs (*arrows*) in the granule neurons of the dentate fascia. The NCIs are not labeled with anti-*TDP-43* antibodies (**b**). Ubiquitin-positive neuropil aggregates and a sparse NCI (*arrow*) in the frontal lobe of an affected 61-year-old female (**c**). *Scale bars* **a**, **b** 50 μm, **c** 10 μm

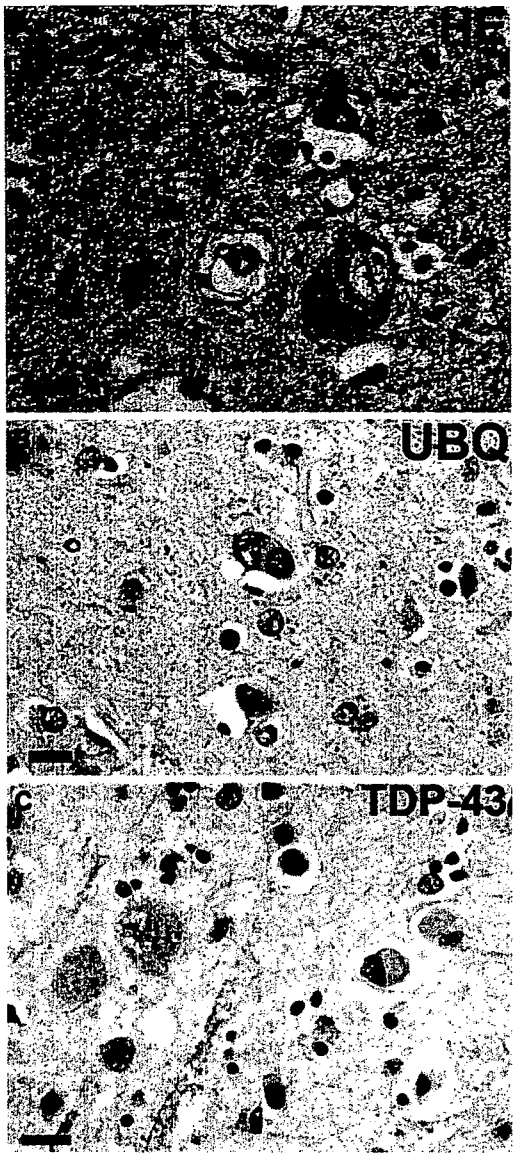

Fig. 13 Basophilic inclusion body disease. **a** A basophilic inclusion (BI) in the precentral gyrus (motor cortex), with a similar, weakly ubiquitin-immunoreactive inclusion in (**b**). **c** Neurons with basophilic inclusions showing fine granular perikaryal *TDP-43* positivity in neurons with BIs on the left and negative in neurons with BIs on the right. **a** Hematoxylin and eosin; **b** ubiquitin, and **c** *TDP-43* immunohistochemistry. *Scale bars* 20 μm

variably ubiquitin-positive, TDP-43-, α-internexin-, α-synuclein-, and tau-negative basophilic inclusions, the most likely neuropathologic diagnosis is basophilic inclusion body disease (BIBD) [58]. If all of the antibodies listed above and routine histological stains such as hematoxylin and eosin fail to reveal signature lesions, and if prion disease has been excluded by IHC or molecular genetics, the remaining FTLD diagnosis is dementia lacking distinctive histologic features (DLDH) [42]. However, it should be borne in mind that in many of the earlier histopathologic surveys, a relatively high proportion of cases of DLDH were encountered [32, 67]. Re-evaluation of such cases using either more sensitive ubiquitin IHC methodologies

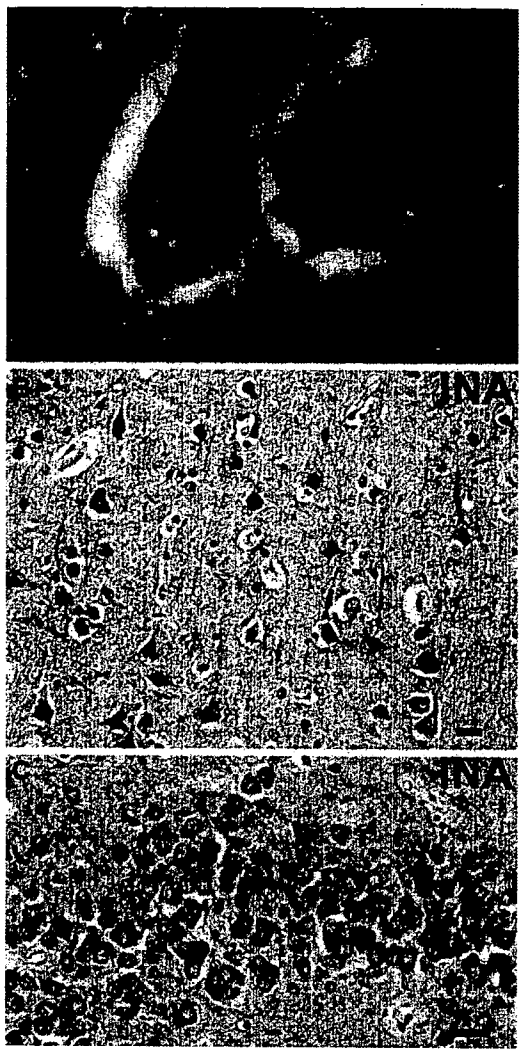

Fig. 14 Neuronal intermediate filament inclusion disease. **a** Eosinophilic Lewy body-like NCI in a pyramidal neuron of the CA1 subfield of the hippocampus. **b** α-Internexin immunoreactive NCIs in layer III of the superior temporal gyrus. **c** Numerous α-internexin immunoreactive NCIs in the granule neurons of the dentate fascia. **a** Hematoxylin and eosin; **b**, **c** α-internexin immunohistochemistry. *Scale bars* 10 μm

[25, 45, 51] or TDP-43 IHC [21] shows DLDH to be an uncommon cause of FTLD and, indeed, it still remains to be proven as a discrete entity with diagnostic criteria other than default characteristics being employed when all IHC and other methods have failed to reveal signature lesions.

Conclusions

The proposed criteria for the neuropathologic diagnosis of FTLD described here are an evolution of the previous criteria described by McKhann et al. [53]. When formulating these proposed criteria, we acknowledged revised staging schemes for other disorders (e.g., AD and DLB), which recommend the use of IHC for the diagnosis of neurodegenerative diseases, replacing silver impregnation methods and averting the lack of reproducibility between centers when these stains are used. We have incorporated the recent identification of new entities into the nosology of FTLD. Most significantly, the discovery of TDP-43 as the major pathologic protein of most forms of FTLD identifies a novel molecular pathology, TDP-43 proteinopathy, and this is now included in the revised criteria. We have also considered the great progress in determining the molecular genetics of FTLD. In addition to FTLD with *MAPT* mutation, other familial subtypes are now recognized on the basis of the neuropathology of ubiquitin and/or TDP-43 IHC, biochemistry, and molecular genetics (FTLD with *PGRN*, *CHMP2B*, and *VCP* mutations, and cases linked to chromosome 9p), which reveal a strong correlation between genotype and neuropathologic phenotype. To facilitate neuropathologic diagnoses of FTLD at research and other centers, commercially available antibodies are now readily available for the identification of the underlying molecular pathologies (e.g., TDP-43 proteinopathy and tauopathy) and the rational diagnosis and nosology of a case of FLTD that comes to autopsy. The neuropathologic diagnostic algorithm described here is based on the current level of knowledge, but the consortium members appreciate that further study of TDP-43 proteinopathy may reveal new subtypes and that other FTLD entities may yet be identified. The proposed neuropathologic algorithm will facilitate efforts to improve the diagnosis of FTLD and encourage multi-center clinico-pathologic studies. Together, these efforts should improve the early and reliable neuropathologic diagnosis of the FTLD, raise the awareness of possible coexisting pathologies, and facilitate research efforts into pathogenesis and potential treatments where none currently exists.

Acknowledgments We thank the clinical, genetic, pathology, and technical staff of the collaborating centers for making information and tissue samples available for this study and we thank the families of patients whose generosity made this research possible. Support for this work was provided by grants from the National Institute on Aging of the National Institutes of Health (P50-AG05681, P01-AG03991, U01-AG16976, P30-AG13854, P30-NS057105, AG10124 and AG17586), the Buchanan Fund, the Winspear Family Center for Research on the Neuropathology of Alzheimer Disease, and the Charles and Joanne Knight Alzheimer Research Initiative.

References

1. Alafuzoff I, Pikkarainen M, Al Sarraj S, Arzberger T, Bell J, Bodi I, Bogdanovic N, Budka H, Bugiani O, Ferrer I, Gelpi E, Giaccone G, Graeber MB, Hauw JJ, Kamphorst W, King A, Kopp N, Korkolopoulou P, Kovacs GG, Meyronet D, Parchi P, Patsouris E, Preusser M, Ravid R, Roggendorf W, Seilhean D, Streichenberger N,

Thal DR, Kretzschmar H (2006) Interlaboratory comparison of assessments of Alzheimer disease-related lesions: a study of the BrainNet Europe Consortium. J Neuropathol Exp Neurol 65:740–757
2. Amador-Ortiz C, Lin W-L, Ahmed Z, Personett D, Davies P, Duara R, Graff-Radford NR, Hutton ML, Dickson DW (2007) TDP-43 immunoreactivity in hippocampal sclerosis and Alzheimer's disease. Ann Neurol 61:435–445
3. Arai T, Hasegawa M, Akiyama H, Ikeda K, Nonaka T, Mori H, Mann D, Tsuchiya K, Yoshida M, Hashizume Y, Oda T (2006) TDP-43 is a component of ubiquitin-positive tau-negative inclusions in frontotemporal lobar degeneration and amyotrophic lateral sclerosis. Biochem Biophys Res Commun 351:602–611
4. Baker M, Mackenzie IR, Pickering-Brown SM, Gass J, Rademakers R, Lindholm C, Snowden J, Adamson J, Sadovnick AD, Rollinson S, Cannon A, Dwosh E, Neary D, Melquist S, Richardson A, Dickson D, Berger Z, Eriksen J, Robinson T, Zehr C, Dickey CA, Crook R, McGowan E, Mann D, Boeve B, Feldman H, Hutton M (2006) Mutations in progranulin cause tau-negative frontotemporal dementia linked to chromosome 17. Nature 442:916–919
5. Behrens MI, Mukherjee O, Tu PH, Liscic RM, Grinberg LT, Carter D, Paulsmeyer K, Taylor-Reinwald L, Gitcho M, Norton JB, Chakraverty S, Goate AM, Morris JC, Cairns NJ (2007) Neuropathologic heterogeneity in HDDD1: a familial frontotemporal lobar degeneration with ubiquitin-positive inclusions and progranulin mutation. Alzheimer Dis Assoc Disord 21:1–7
6. Bigio EH, Lipton AM, Yen SH, Hutton ML, Baker M, Nacharaju P, White CL III, Davies P, Lin W, Dickson DW (2001) Frontal lobe dementia with novel tauopathy: sporadic multiple system tauopathy with dementia. J Neuropathol Exp Neurol 60:328–341
7. Braak H, Braak E (1989) Cortical and subcortical argyrophilic grains characterize a disease associated with adult onset dementia. Neuropathol Appl Neurobiol 15:13–26
8. Braak H, Braak E (1991) Neuropathological stageing of Alzheimer-related changes. Acta Neuropathol 82:239–259
9. Braak H, Ghebremedhin E, Rub U, Bratzke H, Del Tredici K (2004) Stages in the development of Parkinson's disease-related pathology. Cell Tissue Res 318:121–134
10. Braak H, Alafuzoff I, Arzberger T, Kretzschmar H, Del Tredici K (2006) Staging of Alzheimer disease-associated neurofibrillary pathology using paraffin sections and immunocytochemistry. Acta Neuropathol 112:389–404
11. Broe M, Hodges JR, Schofield E, Shepherd CE, Kril JJ, Halliday GM (2003) Staging disease severity in pathologically confirmed cases of frontotemporal dementia. Neurology 60:1005–1011
12. Brun A, Englund B, Gustafson L, Passant U, Mann DMA, Neary D, Snowden JS (1994) Clinical and neuropathological criteria for frontotemporal dementia. J Neurol Neurosurg Psychiatry 57:416–418
13. Buee L, Delacourte A (1999) Comparative biochemistry of tau in progressive supranuclear palsy, corticobasal degeneration, FTDP-17 and Pick's disease. Brain Pathol 9:681–693
14. Cairns NJ, Grossman M, Arnold SE, Burn DJ, Jaros E, Perry RH, Duyckaerts C, Stankoff B, Pillon B, Skullerud K, Cruz-Sanchez FF, Bigio EH, Mackenzie IR, Gearing M, Juncos JL, Glass JD, Yokoo H, Nakazato Y, Mosaheb S, Thorpe JR, Uryu K, Lee VM, Trojanowski JQ (2004) Clinical and neuropathologic variation in neuronal intermediate filament inclusion disease. Neurology 63:1376–1384
15. Cairns NJ, Lee VM, Trojanowski JQ (2004) The cytoskeleton in neurodegenerative diseases. J Pathol 204:438–449
16. Cairns NJ, Neumann M, Bigio EH, Holm IE, Troost D, Hatanpaa KJ, Foong C, White CL III, Schneider JA, Kretzschmar H, Carter D, Taylor-Reinwald L, Paulsmeyer K, Strider J, Gitcho M, Goate AM, Morris JC, Mishra M, Kwong LK, Stieber A, Xu Y, Forman MS, Lee VMY, Trojanowski JQ, Mackenzie IR (2007) TDP-43 in familial and sporadic frontotemporal lobar degeneration with ubiquitin inclusions. Am J Pathol (in press). doi:10.2353/ajpath.2007.070182
17. Ciechanover A, Brundin P (2003) The ubiquitin proteasome system in neurodegenerative diseases: sometimes the chicken, sometimes the egg. Neuron 40:427–446
18. Consensus recommendations for the postmortem diagnosis of Alzheimer's disease. The National Institute on Aging, Reagan Institute Working Group on Diagnostic Criteria for the Neuropathological Assessment of Alzheimer's Disease (1997) Neurobiol Aging 18:S1–S2
19. Cooper PN, Jackson M, Lennox G, Lowe J, Mann DM (1995) Tau, ubiquitin, and alpha B-crystallin immunohistochemistry define the principal causes of degenerative frontotemporal dementia. Arch Neurol 52:1011–1015
20. Cruts M, Gijselinck I, van der Zee J, Engelborghs S, Wils H, Pirici D, Rademakers R, Vandenberghe R, Dermaut B, Martin JJ, van Duijn C, Peeters K, Sciot R, Santens P, De Pooter T, Mattheijssens M, van den Broeck M, Cuijt I, Vennekens K, De Deyn PP, Kumar-Singh S, Van Broeckhoven C (2006) Null mutations in progranulin cause ubiquitin-positive frontotemporal dementia linked to chromosome 17q21. Nature 442:920–924
21. Davidson Y, Kelley T, Mackenzie IR, Pickering-Brown S, Du PD, Neary D, Snowden JS, Mann DM (2007) Ubiquitinated pathological lesions in frontotemporal lobar degeneration contain the TAR DNA-binding protein, TDP-43. Acta Neuropathol 113:521–33
22. de Silva R, Lashley T, Strand C, Shiarli AM, Shi J, Tian J, Bailey KL, Davies P, Bigio EH, Arima K, Iseki E, Murayama S, Kretzschmar H, Neumann M, Lippa C, Halliday G, Mackenzie J, Ravid R, Dickson D, Wszolek Z, Iwatsubo T Pickering-Brown SM, Holton J, Lees A, Revesz T, Mann DM (2006) An immunohistochemical study of cases of sporadic and inherited frontotemporal lobar degeneration using 3R- and 4R-specific tau monoclonal antibodies. Acta Neuropathol 111:329–340
23. Dickson DW, Wertkin A, Kress Y, Ksiezak-Reding H, Yen SH (1990) Ubiquitin immunoreactive structures in normal human brains. Distribution and developmental aspects. Lab Invest 63:87–99
24. Dickson DW, Bergeron C, Chin SS, Duyckaerts C, Horoupian D, Ikeda K, Jellinger K, Lantos PL, Lippa CF, Mirra SS, Tabaton M, Vonsattel JP, Wakabayashi K, Litvan I (2002) Office of Rare Diseases neuropathologic criteria for corticobasal degeneration. J Neuropathol Exp Neurol 61:935–946
25. Forman MS, Farmer J, Johnson JK, Clark CM, Arnold SE, Coslett HB, Chatterjee A, Hurtig HI, Karlawish JH, Rosen HJ, Van Deerlin V, Lee VM, Miller BL, Trojanowski JQ, Grossman M (2006) Frontotemporal dementia: clinicopathological correlations. Ann Neurol 59:952–962
26. Forman MS, Mackenzie IR, Cairns NJ, Swanson E, Boyer PJ, Drachman DA, Jhaveri BS, Karlawish JH, Pestronk A, Smith TW, Tu PH, Watts GD, Markesbery WR, Smith CD, Kimonis VE (2006) Novel ubiquitin neuropathology in frontotemporal dementia with valosin-containing protein gene mutations. J Neuropathol Exp Neurol 65:571–581
27. Gibb WR, Luthert PJ, Marsden CD (1989) Corticobasal degeneration. Brain 112:1171–1192
28. Goedert M, Spillantini MG, Cairns NJ, Crowther RA (1992) Tau proteins of Alzheimer paired helical filaments: abnormal phosphorylation of all six brain isoforms. Neuron 8:159–168
29. Graham A, Davies R, Xuereb J, Halliday G, Kril J, Creasey H, Graham K, Hodges J (2005) Pathologically proven frontotemporal dementia presenting with severe amnesia. Brain 128:597–605
30. Guyant-Marechal L, Laquerriere A, Duyckaerts C, Dumanchin C, Bou J, Dugny F, Le Ber I, Frebourg T, Hannequin D, Campion D (2006) Valosin-containing protein gene mutations: clinical and neuropathologic features. Neurology 67:644–651

31. Hauw JJ, Daniel SE, Dickson D, Horoupian DS, Jellinger K, Lantos PL, McKee A, Tabaton M, Litvan I (1994) Preliminary NINDS neuropathologic criteria for Steele-Richardson-Olszewski syndrome (progressive supranuclear palsy). Neurology 44:2015–2019
32. Hodges JR, Davies RR, Xuereb JH, Casey B, Broe M, Bak TH, Kril JJ, Halliday GM (2004) Clinicopathological correlates in frontotemporal dementia. Ann Neurol 56:399–406
33. Ironside JW, Head MW, Bell JE, McCardle L, Will RG (2000) Laboratory diagnosis of variant Creutzfeldt–Jakob disease. Histopathology 37:1–9
34. Iseki E, Yamamoto R, Murayama N, Minegishi M, Togo T, Katsuse O, Kosaka K, Akiyama H, Tsuchiya K, de Silva R, Lees A, Arai H (2006) Immunohistochemical investigation of neurofibrillary tangles and their tau isoforms in brains of limbic neurofibrillary tangle dementia. Neurosci Lett 405:29–33
35. Jellinger KA, Bancher C (1998) Senile dementia with tangles (tangle predominant form of senile dementia. Brain Pathol 8:367–376
36. Josephs KA, Holton JL, Rossor MN, Godbolt AK, Ozawa T, Strand K, Khan N, Al Sarraj S, Revesz T (2004) Frontotemporal lobar degeneration and ubiquitin immunohistochemistry. Neuropathol Appl Neurobiol 30:369–373
37. Josephs KA, Ahmed Z, Katsuse O, Parisi JF, Boeve BF, Knopman DS, Petersen RC, Davies P, Duara R, Graff-Radford NR, Uitti RJ, Rademakers R, Adamson J, Baker M, Hutton ML, Dickson DW (2007) Neuropathologic features of frontotemporal lobar degeneration with ubiquitin-positive inclusions with progranulin gene (PGRN) mutations. J Neuropathol Exp Neurol 66:142–151
38. Katsuse O, Dickson DW (2005) Ubiquitin immunohistochemistry of frontotemporal lobar degeneration differentiates cases with and without motor neuron disease. Alzheimer Dis Assoc Disord 19(Suppl 1):S37–S43
39. Kersaitis C, Halliday GM, Kril JJ (2004) Regional and cellular pathology in frontotemporal dementia: relationship to stage of disease in cases with and without Pick bodies. Acta Neuropathol 108:515–523
40. Kertesz A, Davidson W, McCabe P, Takagi K, Munoz D (2003) Primary progressive aphasia: diagnosis, varieties, evolution. J Int Neuropsychol Soc 9:710–719
41. Kipps CM, Davies RR, Mitchell J, Kril JJ, Halliday GM, Hodges JR (2007) Clinical significance of lobar atrophy in frontotemporal dementia: application of an MRI visual rating scale. Dement Geriatr Cogn Disord 23:334–342
42. Knopman DS, Mastri AR, Frey WH, Sung JH, Rustan T (1990) Dementia lacking distinctive histologic features: a common non-Alzheimer degenerative dementia. Neurology 40:251–256
43. Knopman DS, Boeve BF, Petersen RC (2003) Essentials of the proper diagnoses of mild cognitive impairment, dementia, and major subtypes of dementia. Mayo Clin Proc 78:1290–1308
44. Lantos PL, Cairns NJ, Khan MN, King A, Revesz T, Janssen JC, Morris H, Rossor MN (2002) Neuropathologic variation in frontotemporal dementia due to the intronic tau 10(+16) mutation. Neurology 58:1169–1175
45. Lipton AM, White CL III, Bigio EH (2004) Frontotemporal lobar degeneration with motor neuron disease-type inclusions predominates in 76 cases of frontotemporal degeneration. Acta Neuropathol 108:379–385
46. Liscic RM, Storandt M, Cairns NJ, Morris JC (2007) Clinical and psychometric distinction of frontotemporal and Alzheimer dementias. Arch Neurol 64:535–540
47. Lowe J (1998) Establishing a pathological diagnosis in degenerative dementias. Brain Pathol 8:403–406
48. Lowe J, Hand N, Mayer RJ (2005) Application of ubiquitin immunohistochemistry to the diagnosis of disease. Methods Enzymol 399:86–119
49. Mackenzie IR, Baborie A, Pickering-Brown S, Plessis DD, Jaros E, Perry RH, Neary D, Snowden JS, Mann DM (2006) Heterogeneity of ubiquitin pathology in frontotemporal lobar degeneration: classification and relation to clinical phenotype. Acta Neuropathol 112:539–549
50. Mackenzie IR, Baker M, Pickering-Brown S, Hsiung GY, Lindholm C, Dwosh E, Gass J, Cannon A, Rademakers R, Hutton M, Feldman HH (2006) The neuropathology of frontotemporal lobar degeneration caused by mutations in the progranulin gene. Brain 129:3081–3090
51. Mackenzie IR, Shi J, Shaw CL, Duplessis D, Neary D, Snowden JS, Mann DM (2006) Dementia lacking distinctive histology (DLDH) revisited. Acta Neuropathol 112:551–559
52. McKeith IG, Dickson DW, Lowe J, Emre M, O'Brien JT, Feldman H, Cummings J, Duda JE, Lippa C, Perry EK, Aarsland D, Arai H, Ballard CG, Boeve B, Burn DJ, Costa D, Del Ser T, Dubois B, Galasko D, Gauthier S, Goetz CG, Gomez-Tortosa E, Halliday G, Hansen LA, Hardy J, Iwatsubo T, Kalaria RN, Kaufer D, Kenny RA, Korczyn A, Kosaka K, Lee VM, Lees A, Litvan I, Londos E, Lopez OL, Minoshima S, Mizuno Y, Molina JA, Mukaetova-Ladinska EB, Pasquier F, Perry RH, Schulz JB, Trojanowski JQ, Yamada M (2005) Diagnosis and management of dementia with Lewy bodies: third report of the DLB Consortium. Neurology 65:1863–1872
53. McKhann GM, Albert MS, Grossman M, Miller B, Dickson D, Trojanowski JQ (2001) Clinical and pathological diagnosis of frontotemporal dementia: report of the Work Group on Frontotemporal Dementia and Pick's Disease. Arch Neurol 58:1803–1809
54. Mirra SS, Heyman A, McKeel D, Sumi SM, Crain BJ, Brownlee LM, Vogel FS, Hughes JP, van Belle G, Berg L (1991) The Consortium to Establish a Registry for Alzheimer's Disease (CERAD). Part II. Standardization of the neuropathologic assessment of Alzheimer's disease. Neurology 41:479–486
55. Momeni P, Schymick J, Jain S, Cookson MR, Cairns NJ, Greggio E, Greenway MJ, Berger S, Pickering-Brown S, Chio A, Fung HC, Holtzman DM, Huey ED, Wassermann EM, Adamson J, Hutton ML, Rogaeva E, George-Hyslop P, Rothstein JD, Hardiman O, Grafman J, Singleton A, Hardy J, Traynor BJ (2006) Analysis of IFT74 as a candidate gene for chromosome 9p-linked ALS-FTD. BMC Neurol. doi:10.1186/1471-2377-6-44
56. Morita M, Al Chalabi A, Andersen PM, Hosler B, Sapp P, Englund E, Mitchell JE, Habgood JJ, de Belleroche J, Xi J, Jongjaroenprasert W, Horvitz HR, Gunnarsson LG, Brown RH Jr (2006) A locus on chromosome 9p confers susceptibility to ALS and frontotemporal dementia. Neurology 66:839–844
57. Mukherjee O, Pastor P, Cairns NJ, Chakraverty S, Kauwe JS, Shears S, Behrens MI, Budde J, Hinrichs AL, Norton J, Levitch D, Taylor-Reinwald L, Gitcho M, Tu PH, Tenenholz GL, Liscic RM, Armendariz J, Morris JC, Goate AM (2006) HDDD2 is a familial frontotemporal lobar degeneration with ubiquitin-positive, tau-negative inclusions caused by a missense mutation in the signal peptide of progranulin. Ann Neurol 60:314–322
58. Munoz DG (1998) The pathology of pick complex. In: Munoz DG (ed) Pick's disease and pick complex. Wiley-Liss, New York, pp 211–241
59. Neary D, Snowden JS, Mann DM, Northen B, Goulding PJ, Macdermott N (1990) Frontal lobe dementia and motor neuron disease. J Neurol Neurosurg Psychiatry 53:23–32
60. Neary D, Snowden JS, Gustafson L, Passant U, Stuss D, Black S, Freedman M, Kertesz A, Robert PH, Albert M, Boone K, Miller BL, Cummings J, Benson DF (1998) Frontotemporal lobar degeneration: a consensus on clinical diagnostic criteria. Neurology 51:1546–1554
61. Neumann M, Sampathu DM, Kwong LK, Truax AC, Micsenyi MC, Chou TT, Bruce J, Schuck T, Grossman M, Clark CM, McCluskey LF, Miller BL, Masliah E, Mackenzie IR, Feldman H, Feiden W, Kretzschmar HA, Trojanowski JQ, Lee VM (2006) Ubiquitinated TDP-43 in frontotemporal lobar degeneration and amyotrophic lateral sclerosis. Science 314:130–133

62. Neumann M, Kwong LK, Truax AC, Vanmassenhove B, Kretzschmar HA, Van Deerlin VM, Clark CM, Grossman M, Miller BL, Trojanowski JQ, Lee VM (2007) TDP-43-positive white matter pathology in frontotemporal lobar degeneration with ubiquitin-positive inclusions. J Neuropathol Exp Neurol 66:177–183
63. Neumann M, Mackenzie IR, Cairns NJ, Boyer PJ, Markesbery WR, Smith CD, Taylor JP, Kretzschmar HA, Kimonis VE, Forman MS (2007) TDP-43 in the ubiquitin pathology of frontotemporal dementia with VCP gene mutations. J Neuropathol Exp Neurol 66:152–157
64. Okamoto K, Hirai S, Yamazaki T, Sun XY, Nakazato Y (1991) New ubiquitin-positive intraneuronal inclusions in the extra-motor cortices in patients with amyotrophic lateral sclerosis. Neurosci Lett 129:233–236
65. Rossor MN, Revesz T, Lantos PL, Warrington EK (2000) Semantic dementia with ubiquitin-positive tau-negative inclusion bodies. Brain 123:267–276
66. Sampathu DM, Neumann M, Kwong LK, Chou TT, Micsenyi M, Truax A, Bruce J, Grossman M, Trojanowski JQ, Lee VM (2006) Pathological heterogeneity of frontotemporal lobar degeneration with ubiquitin-positive inclusions delineated by ubiquitin immunohistochemistry and novel monoclonal antibodies. Am J Pathol 169:1343–1352
67. Shi J, Shaw CL, Du PD, Richardson AM, Bailey KL, Julien C, Stopford C, Thompson J, Varma A, Craufurd D, Tian J, Pickering-Brown S, Neary D, Snowden JS, Mann DM (2005) Histopathological changes underlying frontotemporal lobar degeneration with clinicopathological correlation. Acta Neuropathol 110:501–512
68. Skibinski G, Parkinson NJ, Brown JM, Chakrabarti L, Lloyd SL, Hummerich H, Nielsen JE, Hodges JR, Spillantini MG, Thusgaard T, Brandner S, Brun A, Rossor MN, Gade A, Johannsen P, Sorensen SA, Gydesen S, Fisher EM, Collinge J (2005) Mutations in the endosomal ESCRTIII-complex subunit CHMP2B in frontotemporal dementia. Nat Genet 37:806–808
69. Snowden JS, Neary D, Mann DM (2002) Frontotemporal dementia. Br J Psychiatry 180:140–143
70. Spillantini MG, van Swieten JC, Goedert M (2000) Tau gene mutations in frontotemporal dementia and parkinsonism linked to chromosome 17 (FTDP-17). Neurogenetics 2:193–205
71. Srinivasan R, Davidson Y, Gibbons L, Payton A, Richardson AM, Varma A, Julien C, Stopford C, Thompson J, Horan MA, Pendleton N, Pickering-Brown SM, Neary D, Snowden JS, Mann DM (2006) The apolipoprotein E epsilon 4 allele selectively increases the risk of frontotemporal lobar degeneration in males. J Neurol Neurosurg Psychiatry 77:154–158
72. Steele JC, Richardson JC, Olszewski J (1964) Progressive supranuclear palsy. A heterogeneous degeneration involving the brain stem, basal ganglia and cerebellum with vertical gaze and pseudobulbar palsy, nuchal dystonia and dementia. Arch Neurol 10:333–359
73. Taniguchi S, McDonagh AM, Pickering-Brown SM, Umeda Y, Iwatsubo T, Hasegawa M, Mann DM (2004) The neuropathology of frontotemporal lobar degeneration with respect to the cytological and biochemical characteristics of tau protein. Neuropathol Appl Neurobiol 30:1–18
74. Togo T, Sahara N, Yen SH, Cookson N, Ishizawa T, Hutton M, de Silva R, Lees A, Dickson DW (2002) Argyrophilic grain disease is a sporadic 4-repeat tauopathy. J Neuropathol Exp Neurol 61:547–556
75. Vance C, Al Chalabi A, Ruddy D, Smith BN, Hu X, Sreedharan J, Siddique T, Schelhaas HJ, Kusters B, Troost D, Baas F, de Jong V, Shaw CE (2006) Familial amyotrophic lateral sclerosis with frontotemporal dementia is linked to a locus on chromosome 9p13.2-21.3. Brain 129:868–876
76. van der Knaap MS, Naidu S, Kleinschmidt-Demasters BK, Kamphorst W, Weinstein HC (2000) Autosomal dominant diffuse leukoencephalopathy with neuroaxonal spheroids. Neurology 54:463–468
77. Watts GD, Wymer J, Kovach MJ, Mehta SG, Mumm S, Darvish D, Pestronk A, Whyte MP, Kimonis VE (2004) Inclusion body myopathy associated with Paget disease of bone and frontotemporal dementia is caused by mutant valosin-containing protein. Nat Genet 36:377–381
78. Weintraub S, Rubin NP, Mesulam MM (1990) Primary progressive aphasia. Longitudinal course, neuropsychological profile, and language features. Arch Neurol 47:1329–1335
79. Wightman G, Anderson VER, Martin J, Swash M, Anderton BH, Neary D, Mann D, Luthert P, Leigh PN (1992) Hippocampal and neocortical ubiquitin-immunoreactive inclusions in amyotrophic-lateral-sclerosis with dementia. Neurosci Lett 139:269–274
80. Zhukareva V, Mann D, Pickering-Brown S, Uryu K, Shuck T, Shah K, Grossman M, Miller BL, Hulette CM, Feinstein SC, Trojanowski JQ, Lee VM (2002) Sporadic Pick's disease: a tauopathy characterized by a spectrum of pathological tau isoforms in gray and white matter. Ann Neurol 51:730–739

Neuropathology 2007; **27**, 578–584 doi:10.1111/j.1440-1789.2007.00806.x

Symposium: Brain imaging and neuropathology

Neuropathology of mild cognitive impairment

Yuko Saito[1] and Shigeo Murayama[2]

[1]Department of Pathology, Tokyo Metropolitan Geriatric Hospital, and [2]Department of Neuropathology, Tokyo Metropolitan Institute of Gerontology, Tokyo, Japan

We aim to investigate the pathological background of mild cognitive impairment (MCI). The most recent 545 cases from the Brain Bank for Aging Research (BBAR) were studied, with a mean age of 80.7 years and male : female ratio of 324 : 221. Cases with clinical dementia rating scale (CDR) 0.5 were retrieved as the best substitute of MCI. CDR was retrospectively determined from clinical charts. Pathological examinations followed the BBAR protocol (JNEN 2004). Post mortem assessment of CDR was possible for 486 cases, and was 0 in 201 cases, 0.5 in 57 cases and 1–3 in 228 cases. CDR 0.5 group was clinicopathologically classified into 33 cases with degenerative changes, nine cases with vascular changes, four cases with combined degenerative and vascular changes, two with hippocampal sclerosis, two with trauma, one with metabolic disease and six with unremarkable changes. The degenerative group was further subclassified into groups with pure and combined pathology. The former consisted of six cases each with Alzheimer change (AC), argyrophilic grain change (AGC) and neurofibrillary tangle predominant change (NFTC), three each with Lewy body disease change without parkinsonism (DLBC) or Parkinson's disease (PDMCI) and one case with progressive supranuclear palsy. The latter consisted of three cases with AC plus AGC, two with AGC plus NFTC and one each with AC plus DLBC, DLBC plus amyotrophic lateral sclerosis and AGC plus DLBC. The pathological backgrounds of patients of class CDR 0.5 were varied and not restricted to AC.

Key words: amyloid β, argyrophilic grains, α-synuclein, clinical dementia rating scale, tauopathy.

Correspondence: Yuko Saito, MD, PhD. Department of Neuropathology, Tokyo Metropolitan Insitute of Gerontology, 25-2 Sakaecho, Itabashi-ku, Tokyo, Japan. Email: yukosa@tmig.or.jp

Received 26 November 2006; revised and accepted 26 December 2006.

INTRODUCTION

The concept of mild cognitive impairment (MCI) was proposed for the selection of the most vulnerable populations regarding the progression to dementia and to aid in the development of efficient early interventions. However, the concept remains controversial because it lacks the insight into the pathological background, or it has been expanded to encompass more cases than the original definition.

The clinical dementia rating scale (CDR)[1] was originally proposed for use in the objective evaluation of cognitive function, and later refined extensively regarding methodological points, and has now been adapted reliably for retrospective analysis. CDR 0.5 was the original requirement for MCI, and is thought to be the best reliable substitute for MCI[2] in retrospective studies.

In this study, the most recent serial autopsy cases of the Brain Bank for Aging Research (BBAR) were employed. The cases roughly represent an aging cohort of the Tokyo suburban area and are quite distinct from cases from memory clinics, whose chief complaints are amnesia. The results obtained here indicate that the pathology associated with CDR 0.5 was variable in a general aged population.

MATERIALS AND METHODS

Tissue source

Five hundred and forty-five serial autopsy brains from the BBAR were employed for this study. They consisted of consecutive autopsy cases from a general geriatric hospital providing community care, including full-time emergent medical service. The patients' ages ranged from 48 to 104 years, with a mean age of 80.7 ± 8.8 years, and the male : female ratio was 324 : 221.

Clinical information

Intellectual activity of daily living (IADL) was evaluated at discharge by attending nurses. The Mini-Mental State

Examination (MMSE)[3] and/or Hasegawa dementia scale[4,5] were included in clinical charts and conducted by attending physicians at admission. Two board-certified neurologists read the entire clinical records and determined CDR independently.[1] If the information in the clinical chart was not sufficient to determine CDR, interviews with the patients' attending physicians or caregivers were added to determine CDR. The results were recorded in the BBAR data base.

Selection of CDR 0.5 cases

The CDR 0.5 cases were selected from the BBAR database. All cases were reviewed again and the description of any memory disturbance that interfered with clinical intervention was confirmed in the clinical charts. In order to eliminate possible influence from systemic disorders, those CDR 0.5 cases with serious medical conditions at evaluation of cognitive state were excluded from the study.

Neuropathology

All serial autopsy cases were examined with the BBAR protocol described below, irrespective of clinical diagnosis.[6,7] At autopsy, after taking photos of the whole brain, the non-dominant hemisphere or the hemisphere spared from focal lesions was serially sectioned at 7-mm thickness. The cerebrum was cut on the coronal plane, the brain stem on the axial plane, and the cerebellum on the sagittal plane. Photos were taken of all slices. Small pieces of the anterior amygdala, posterior hippocampus, frontal, temporal and occipital poles, supramarginal gyrus and rostral midbrain were directly fixed in 4% paraformaldehyde for 48 h and prepared for immunohistochemical and ultrastructural studies. The remaining slices were quick frozen and stored at –80°C. The hemisphere kept for morphological examinations was fixed in 20% neutral buffered formalin for 7–13 days and cut into 7-mm thick sections, similar to the contralateral hemisphere. Serial coronal sections of the cerebrum, axial sections of the brain stem, and sagittal sections of the cerebellum, together with the photos of the serial sections of the contralateral hemisphere were carefully compared with CT, MRI, single photon emission computed tomography (SPECT) and positron emission tomography (PET) images whenever available and correlated with clinical findings, including CSF biomarkers.

Paraffin-embedded sections of representative areas of the brain were examined. The selected anatomical structures included those recommended by the Consortium to Establish a Registry for Alzheimer Disease (CERAD),[8] the Consensus Guidelines for the Diagnosis of Dementia with Lewy Bodies (DLB),[9] Braak and Braak recommendation,[10] and Diagnostic Criteria of Progressive Supranuclear Palsy.[11] These included the frontal pole, temporal pole, cingulate gyrus, second frontal gyrus, accumbence and septal nuclei, amygdala, basal nucleus of Meynert, second temporal gyrus, anterior hippocampus with entorhinal and transentorhinal cortex, basal ganglia and hypothalamus with mamillary body, subthalamic nucleus, posterior hippocampus, thalamus with red nucleus, motor cortex, parietal lobe with intraparietal sulcus, visual cortex, midbrain, upper and middle pons, medulla oblongata, cerebellar vermis, dentate nucleus, and multiple cervical, thoracic, and lumbar levels of the spinal cord.

Six-micrometer-thick sections were routinely stained with HE and Klüver-Barrera method. Selected sections were stained with the modified methenamine,[12] Gallyas-Braak[13] and Bielschowsky silver staining for senile changes, with Congo red for amyloid β deposition, and with elastica Masson trichrome staining for vascular changes.

Immunohistochemistry

Six-micrometer-thick serial sections were immunohistochemically stained, using a Ventana 20NX autostainer (Ventana, Tucson, AZ, US), as previously described.[6,7] The antibodies applied to all the cases were: antiphosphorylated α-synuclein (psyn) (psyn#64[14]); phosphorylated tau (ptau) (AT8, monoclonal, Innogenetic, Temse, Belgium); amyloid β (Aβ) 11–28 (12B2, monoclonal, IBL, Maebashi, Japan); and ubiquitin (polyclonal, DAKO, Glostrup, Denmark). Selected cases were also examined with antibodies to: non-phosphorylated α-synuclein (LB509, a gift from Dr Iwatsubo); phosphorylataed α-synuclein (polyclonal, Pser 129); Aβ 1–42 (polyclonal, IBL); glial fibrillary acidic protein (GFAP) (polyclonal, DAKO, Glostrup, Denmark); HLA-DR (monoclonal, CD68, DAKO, Glostrup, Denmark); phosphorylated neurofilament (monoclonal SMI31, Sternberger Immunochemical, Baltimore, MO, US); and myelin basic proteins (polyclonal, DAKO, Glostrup, Denmark).

Semiquantitive evaluation of senile changes

Lewy body (LB) pathology was classified into six LB stages as previously described.[6,15] NFT pathology was classified into Braak's seven stages, and senile plaque (SP) into his four stages.[10] Arygyrophilic grains (AGs) were categorized into four stages as previously specified.[7] Amyloid angiopathy was classified into four stages using our criteria.[16]

Neuropathological diagnostic criteria for dementing disorders

Our modification[17] of the NIA-Regan criteria[18] was used for the diagnosis of Alzheimer's disease (AD): NFT stage ≥IV and SP stage = C. Cases were classified into "Early AD" when SP stage was ≥B and NFT stage was ≥III,

excluding AD cases as defined above. The diagnosis of dementia with Lewy bodies (DLB) was based on the first consensus guideline of DLB.[9] The diagnoses of "dementia with grains" (DG) and "neurofibrillary tangle-predominant form of dementia" (NFTD) were based on Jellinger's criteria.[19,20] Namely, DG presented with AG as the only explainable cause for dementia and NFTD as an excessive amount of NFTs in the hippocampus and SP stage comparable to age-matched controls. From the study of demented cases presenting with pure pathology, we adopted AG Stage III as DG and NFT stage III or IV and SP stage ≤ A as NFTD. The diagnosis of vascular dementia (VD) was based on the NINDS-AIREN criteria.[21] In addition, cases with definite strategic infarcts, multiple infarcts mainly involving gray matter and progressive subcortical leukoencephalopathy "Binswanger type" were included in VD. The diagnosis of "hippocampal sclerosis" was given to cases with marked neuronal loss and variable grade of gliosis in the CA1 of hippocampus, without other explainable changes.

Neuropathological diagnosis for CDR 0.5

CDR 0.5 cases were classified following the neuropathological diagnostic criteria for dementia described above. AC included pathological changes of AD and early AD. AGC was specified as its stage ≥ stage II.[7] NFTC was diagnosed when the pathological changes fulfilled the above criteria for NFTD. DLBC was diagnosed when the cases fulfilled the above criteria for DLB. "Hippocampal sclerosis" followed the above morphological description of "hippocampal sclerosis".

ApoE gyenotyping

Genomic DNA was extracted from the kidneys which had been snap-frozen at autopsy and apoE genotyping was performed with PCR, as previously reported.[22] The typing was successfully completed in 462 out of 545 cases.

RESULTS

Clinical profiles

Clinical dementia ratings were available in 486 cases (89%) as follows: CDR 0 = 201 cases, CDR 0.5 = 57 cases, CDR 1 = 96 cases, CDR 2 = 31 cases, and CDR 3 = 101 cases.

Neuropathological diagnosis of CDR 0.5 cases, in comparison with demented cases

The neuropathological diagnosis of cases with CDR 0.5 was as follows. Thirty-three cases (57%) presented with mainly neurodegenerative pathology, nine cases (15%) with mainly vascular pathology, four (7%) with combined neurodegenerative and vascular etiologies, two (4%) with hippocampal sclerosis, two (4%) with cerebral contusion, one with metabolic encephalopathy, and six (11%) with neuropathologically unremarkable findings (Fig. 1A).

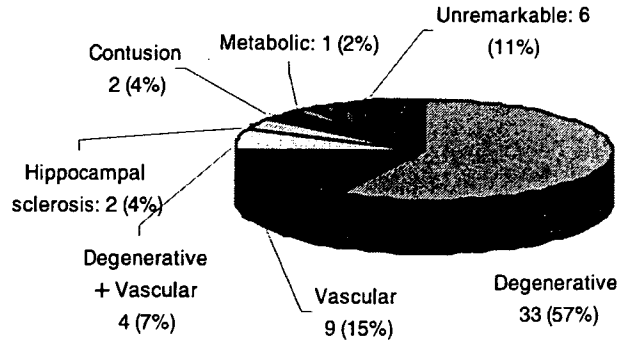

Fig. 1 Neuropathology of with clinical dementia rating scale (CDR) 0.5 and CDR ≥ 1. (A) Neuropathology of CDR 0.5. Degenerative background (64%) was approximately three times more frequent than vascular background (22%), when those cases with combined degenerative and vascular pathology were counted twice to be included into both categories. Each number represents the number of cases. (B) Neuropathology of CDR ≥ 1. Degenerative dementia (60%) was two-fold more frequent than vascular dementia (32%).

The neuropathological diagnosis of cases with dementia (CDR1–3) was as follows. One hundred and thirty cases (57%) showed neurodegenerative pathology: 64 cases (28%) vascular pathology; nine (4%) combined neurodegenerative and vascular pathology; six (3%) Creutzfeldt Jacob disease; seven (3%) metabolic encephalopathy; four (2%), cerebral contusion; and one neuropathologically unremarkable changes.

The neurodegenerative pathology of CDR 0.5 cases was further subclassified as follows: six cases (19%) of AC; six (18%) of AGC; six (18%) of NFTC; three of DLBC; three (9%) of Parkinson's disease; one (3%) of PSP; three (9%) of AC plus AGC; one of AC plus DLBC; two (6%) of AGC plus NFTC; one of DLBC plus ALS; and one (3%) of AGC plus DLBC (Fig. 2A). In summary, AC was found in 31%, AGC in 36%, NFTC in 25%, and DLBC in 18% of CDR 0.5 cases.

The neurodegenerative pathology of dementia (CDR1–3) was classified as follows: 44 cases (34%) of AD; 22 (17%) of DLB; 15 (12%) of DG; nine (7%) of AD plus DLB; nine (7%) of PSP; six (5%) of NFTD; four (3%) of ALS; four (3%) of DG plus NFTD; two (2%) of AD plus DG; one (1%) of Pick disease; one (1%) of Huntington disease; one of DLB plus PSP plus DG; one of DLB plus diffuse neurofibrillary tangles with calcification; one of corticobasal degeneration plus DG; and one of DG plus PSP (Fig. 2B). In total, AD was found in 45%, DLB was found in 26% and DG was found in 18% of the cases with dementia.

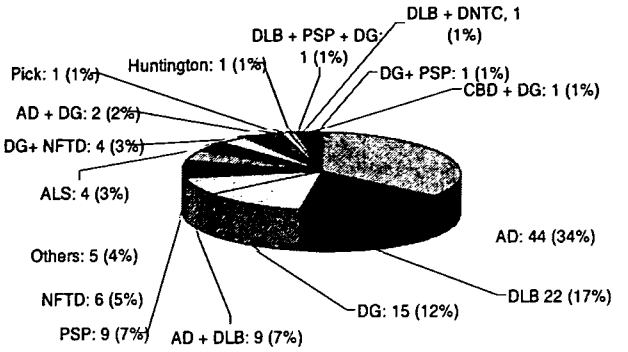

Fig. 2 Detailed degenerative pathology of with clinical dementia rating scale (CDR) 0.5 and CDR ≥ 1. (A) Degenerative pathology in CDR 0.5 consisted of 36% argyrophilic grain change (AGC), 31% Alzheimer change (AC), 24% the neurofibrillary tangle predominant change (NFTC) and 9% dementia with Lewy body disease change (DLBC). Those cases with combined degenerative pathology, for example, AC + DLBC, were counted twice to be included in both categories AC and DLBC. (B) Degenerative pathology in CDR ≥ 1 consisted of 43% Alzheimer's disease (AD), 26% dementia with Lewy bodies (DLB), 12% dementia with grain (DG) and 11% neurofibrillary tangle predominant form of dementia (NFTD). The higher frequency of AD and DLB among CDR ≥ 1, than that of AC and DLBC among CDR 0.5, could be best explained by faster speed of exacerbation in these two groups, in AGC and NFTC.

Table 1 Case profiles of CDR 0.5 with pure Alzheimer change

Age/ gender	Brain weight (g)	Stages of senile changes				ApoE genotyping
		NFT	SP	LB	AG	
82/F	1070	III	C	0	0	34
88/F	1030	III	C	0	0	34
88/M	1370	III	B	0	0	33
91/M	1155	III	C	0	0	34
94/F	1550	III	B	0	1	33
94/F	1080	III	B	0	2	33

SP, senile plaque; LB, Lewy body; AG, arygyrophilic grain; NFT, SP: Braak stage.[10] LB, AG: our stage.[6,7]

Senile tauopathy

We define "senile tauopathy" as tauopathy independent from Aβ accumulation, which includes argyrophilic grain disease (AGD), neurofibrillary tangle predominant disease (NFTD), progressive supranuclear palsy (PSP), corticobasal degeneration (CBD), diffuse neurofibrillary tangle disease with calcification (DNTC) and other unclassified tauopathy. PSP and CBD are classified into Parkinson's disease-related disorders, but in the aged cohort, their initial symptoms could be cognitive decline and these cases should instead be classified as senile tauopathy. Clinical characterization of AGD and NFTD is still underway, because they are often complicated with each other and also coexist with PSP or CBD.

Table 2 Case profiles of CDR 0.5 with pure argyrophilic grain disease (AGD)

Age/ gender	Brain weight (g)	Stages of senile changes				ApoE genotyping
		NFT	SP	LB	AG	
78	1150	II	A	1	3	34
80	1180	I	B	1	3	33
86	1177	II	B	1	3	33
93	1185	I	B	0	2	33
93	1190	II	A	0.5	2	33
94	1451	II	A	1	3	ND

SP, senile plaque; LB, Lewy body; AG, arygyrophilic grain; NFT, SP: Braak stage.[10] LB, AG: our stage.[6,7]

Table 3 Case profiles of CDR 0.5 with pure neurofibrillary tangle predominant change

Age/ gender	Brain weight (g)	Stages of senile changes				ApoE genotyping
		NFT	SP	LB	AG	
88/M	1130	III	A	0	0	33
89/F	1221	IV	0	0	0	34
91/M	1090	IV	0	1	1	33
93/F	1100	III	0	0	0	33
99/F	1200	III	A	0	0	33

SP, senile plaque; LB, Lewy body; AG, arygyrophilic grain; NFT, SP: Braak stage.[10] LB, AG: our stage.[6,7]

Table 4 Case profiles of CDR 0.5 with pure "dementia with Lewy body" change

Age/ gender	Brain weight (g)	Stages of senile changes				ApoE genotyping
		NFT	SP	LB	AG	
82/F†	973	I	0	2 (3‡)	0	33
88/M	1235	I	A	2 (3‡)	1	33
90/F	981	II	A	2 (5‡)	0	33

SP, senile plaque; LB, Lewy body; AG, arygyrophilic grain; NFT, SP: Braak stage.[10] LB, AG: our stage.[6,7]

†A history of delusion during her stay in the hospital. ‡Lewy body scores, defined by the first Consensus Guideline of Dementia with Lewy bodies.[9]

In this cohort, senile tauopathy was found among 57% of CDR0.5 cases and 33% of demented cases.

Case profiles of CDR 0.5 with single pathology

Alzheimer change in CDR 0.5

The case profiles are summarized in Table 1. The mean age was 89.5 years. All cases fulfilled the criteria of "early AD". The allelic frequency of apoE ε4 was 25%, which was higher than that in the total cases (10.1%).

Argyrophilic grain change in CDR 0.5

The case profiles are summarized in Table 2. The mean age was 87.3 years. Four of the six cases (67%) showed abundant AGs, fulfilling the criteria for dementia with grains.[7]

Table 5 Case profiles of CDR 0.5 with "hippocampal sclerosis"

Age/ gender	Brain weight (g)	Stages of senile changes				CVD lesion	Atherosclerosis
		NFT	SP	LB	AG		
94/F	850	II	0	0	1	–	Mild
89/M	1296	0	B	0	0	–	Mild

SP, senile plaque; LB, Lewy body; AG, arygyrophilic grain; CVD, cardiovascular disease; NFT, SP: Braak stage.[10] LB, AG: our stage.[6,7]

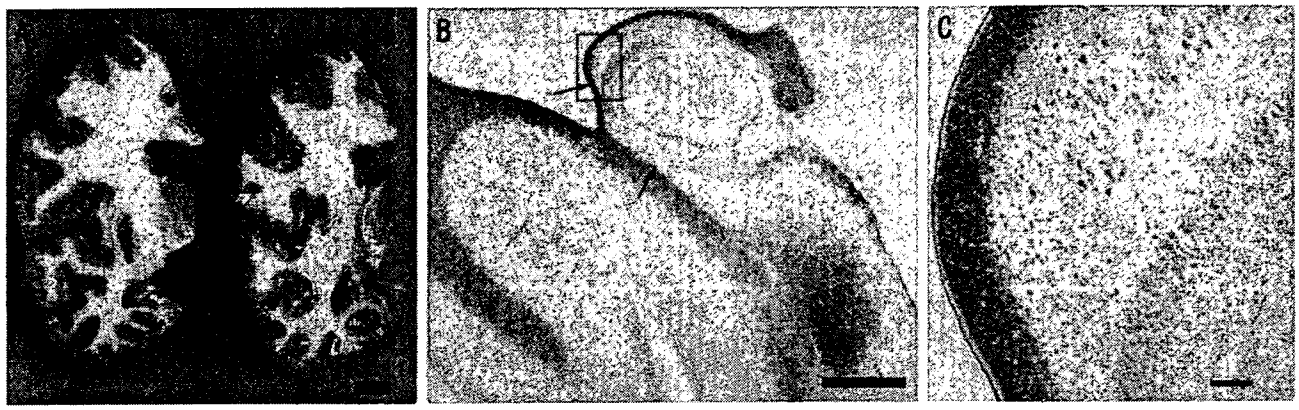

Fig. 3 Neuropathology of hippocampal sclerosis. (A) Macroscopic pathology of hippocampal sclerosis with serial unfixed coronal sections. Prominent atrophy of posterior hippocampus (bar = 1 cm). (B) Myelin-stained sections, demonstrating marked atrophy involving the CA1 and the subiculum (arrows). (Klüver-Barrera stain, bar = 0.5 cm). (C) Higher magnification of the hippocampus, indicated by a rectangle in section B, showing severe neuronal loss of CA1, relatively sparing CA2 (Klüver-Barrera stain, bar = 100 μm).

Neurofibrillary tangle predominant change in CDR 0.5

The case profiles are summarized in Table 3. The mean age of this group was highest (91.6 years).

Dementia with Lewy bodies – type change in CDR 0.5

The case profiles are summarized in Table 4. All cases showed amnesia as the chief complaint. All cases exhibited the presence of cortical Lewy bodies, fulfilling DLB limbic type.

Hippocampal sclerosis in CDR 0.5

The case profiles are summarized in Table 5. Both cases showed degeneration restricted to the anterior to posterior hippocampus (Fig. 3) without degenerative or vascular changes.

Neuropathologically unremarkable cases in CDR 0.5

The case profiles are summarized in Table 6. There was one case accompanied with severe compression myelopathy causing a bed-ridden state.

DISCUSSION

This study examined the pathological background of CDR 0.5 cases from serial autopsy cases from a general geriatric hospital, which roughly represent a general geriatric cohort. The results showed considerable differences from those obtained in memory clinics, where cases with AD represent the majority.

Table 6 Case profiles of CDR 0.5 without specific neuropathological changes

Age/ gender	Brain weight (g)	Stages of senile changes				ApoE genotyping
		NFT	SP	LB	AG	
76/F	1175	II	A	0	1	33
76/F	1280	I	A	0	0	33
79/M	1180	II	0	0	0	33
95/M	1032	II	B	0	0	34
97/F†	969	I	B	0	0	33

SP, senile plaque; LB, Lewy body; AG, arygyrophilic grain; NFT, SP: Braak stage.[10] LB, AG: our stage.[6,7]

†Bedridden state due to cervical compression myelopathy.

The pathological background of CDR 0.5 in our series consisted of AC, AGC, NFTC and DLBC, as well as vascular change and trauma. Special mention should be made of hippocampal sclerosis, which in Japan, has been neglected as secondary hypoxic/ischemic changes. Since these patients apparently survived the hypoxic/ischemic insults causing hippocampal sclerosis in recent advanced medical care, this pathology should be considered as a cause of cognitive decline, as stressed in the US.

A considerable number of cases showed non-specific pathology, making it difficult to explain the cognitive

decline. These cases may represent depression or reversible MCI. Many CDR 0.5 cases presented with various pathologies and it was difficult to determine which pathology most strongly contributed to cognitive decline with this type of retrospective study. Nevertheless, this study of cases with single neuropathological alterations definitely demonstrates that there were multiple pathological bases for CDR 0.5.

When the pathological background of CDR 0.5 was compared with that of dementia, they both shared each pathological component, but the incidences were different. The reason why the frequency of senile tauopathy was higher in CDR 0.5 than in CDR ≥1 was probably related to the speed in the progression of cognitive decline. In other words, AC/DLBC groups progress rapidly, while AGD/NFTC groups present with a more benign course, and thus the latter stay in CDR 0.5 longer. We are now examining cases of CDR 0.5 with MRI VSRAD, CSF biomarkers and PET scan, including fluorodeoxyglucose (FDG) and Pittsburgh Compound B (PIB). The results show that the cases presenting with normal Aβ 42 in the CSF and lacking cerebral cortical deposition of PIB show a slowly progressing course (data not shown).

From clinical longitudinal studies, MCI cases were classified into progressive, non-progressive and recovering subgroups. Our pathological study indicates that the first group may represent an AC/DLBC group, the second, an AGC/NFTC group and the last, unremarkable pathology.

Recently, neuropathological studies of mild cognitive impairment and cases of dementia followed from MCI stages were reported from the longitudinal prospective studies.[23,24] The results were similar to our findings, with highest frequency of AD, but definitely included cases of AGC/NFTC changes.

Our study confirmed that MCI or CDR 0.5 represents a stage of cognitive decline and can be explained by different pathological backgrounds. So MCI or CDR 0.5 should receive a diagnosis of early AD, DLB, DG, NFTD, VD or unremarkable pathology and the most appropriate method for intervention should be employed. For this purpose, we are now conducting multi-institutional prospective longitudinal studies.

REFERENCES

1. Hughes CP, Berg L, Danziger WL, Coben LA, Martin RL. A new clinical scale for the staging of dementia. *Br J Psychiatry* 1982; **140**: 566–572.
2. Petersen RC, Smith GE, Waring SC, Ivnik RJ, Tangalos EG, Kokmen E. Mild cognitive impairment: clinical characterization and outcome. *Arch Neurol* 1999; **56**: 303–308.
3. Folstein MF, Folstein SE, McHugh PR. "Mini-mental state". A practical method for grading the cognitive state of patients for the clinician. *J Psychiatr Res* 1975; **12**: 189–198.
4. Hasegawa K, Inoue K, Moriya K. An investigation of dementia rating scale for the elderly. *Seishin Igaku* 1974; **16**: 965–969.
5. Katoh S, Simogaki H, Onodera A *et al.* Development of the revised version of Hasegawa's dementia scale (HDS-R). *Ronen Seisin Igaku Zassi* 1991; **2**: 1339–1347.
6. Saito Y, Ruberu NN, Sawabe M *et al.* Lewy body-related alpha-synucleinopathy in aging. *J Neuropathol Exp Neurol* 2004; **63**: 742–749.
7. Saito Y, Ruberu NN, Sawabe M *et al.* Staging of argyrophilic grains: an age-associated tauopathy. *J Neuropathol Exp Neurol* 2004; **63**: 911–918.
8. Mirra SS, Heyman A, McKeel D *et al.* The Consortium to Establish a Registry for Alzheimer's Disease (CERAD). Part II. Standardization of the neuropathologic assessment of Alzheimer's disease. *Neurology* 1991; **41**: 479–486.
9. McKeith IG, Galasko D, Kosaka K *et al.* Consensus guidelines for the clinical and pathologic diagnosis of dementia with Lewy bodies (DLB): report of the consortium on DLB international workshop. *Neurology* 1996; **47**: 1113–1124.
10. Braak H, Braak E. Neuropathological stageing of Alzheimer-related changes. *Acta Neuropathol (Berl)* 1991; **82**: 239–259.
11. Hauw JJ, Daniel SE, Dickson D *et al.* Preliminary NINDS neuropathologic criteria for Steele–Richardson–Olszewski syndrome (progressive supranuclear palsy). *Neurology* 1994; **44**: 2015–2019.
12. Yamaguchi H, Haga C, Hirai S, Nakazato Y, Kosaka K. Distinctive, rapid, and easy labeling of diffuse plaques in the Alzheimer brains by a new methenamine silver stain. *Acta Neuropathol (Berl)* 1990; **79**: 569–572.
13. Gallyas F. Silver staining of Alzheimer's neurofibrillary changes by means of physical development. *Acta Morphol Acad Sci Hung* 1971; **19**: 1–8.
14. Fujiwara H, Hasegawa M, Dohmae N *et al.* alpha-Synuclein is phosphorylated in synucleinopathy lesions. *Nat Cell Biol* 2002; **4**: 160–164.
15. Saito Y, Kawashima A, Ruberu NN *et al.* Accumulation of phosphorylated alpha-synuclein in aging human brain. *J Neuropathol Exp Neurol* 2003; **62**: 644–654.
16. Hatsuta H, Saito Y, Ikemura M *et al.* Extension staging criteria of cerebral amyloid angiopathy. *Neuropathology* 2006; **26**: A9.
17. Murayama S, Saito Y. Neuropathological diagnostic criteria for Alzheimer's disease. *Neuropathology* 2004; **24**: 254–260.

18. The National Institute on Aging, and Reagan Institute Working Group on Diagnostic Criteria for the Neuropathological Assessment of Alzheimer's Disease. Consensus recommendations for the postmortem diagnosis of Alzheimer's disease. *Neurobiol Aging* 1997; **18** (4 Suppl): S1–S2.
19. Jellinger KA. Dementia with grains (argyrophilic grain disease). *Brain Pathol* 1998; **8**: 377–386.
20. Jellinger KA, Bancher C. Senile dementia with tangles (tangle predominant form of senile dementia). *Brain Pathol* 1998; **8**: 367–376.
21. Roman GC, Tatemichi TK, Erkinjuntti T *et al.* Vascular dementia: diagnostic criteria for research studies. Report of the NINDS-AIREN International Workshop. *Neurology* 1993; **43**: 250–260.
22. Saito Y, Nakahara K, Yamanouchi H, Murayama S. Severe involvement of ambient gyrus in dementia with grains. *J Neuropathol Exp Neurol* 2002; **61**: 789–796.
23. Jicha GA, Parisi JE, Dickson DW *et al.* Neuropathologic outcome of mild cognitive impairment following progression to clinical dementia. *Arch Neurol* 2006; **63**: 674–681.
24. Petersen RC, Parisi JE, Dickson DW *et al.* Neuropathologic features of amnestic mild cognitive impairment. *Arch Neurol* 2006; **63**: 665–672.

Journal of Neuroscience Research 85:3098–3108 (2007)

Molecular Chaperone-Mediated Tau Protein Metabolism Counteracts the Formation of Granular Tau Oligomers in Human Brain

N. Sahara,[1]* S. Maeda,[1] Y. Yoshiike,[1] T. Mizoroki,[1] S. Yamashita,[1] M. Murayama,[1] J.-M. Park,[1] Y. Saito,[2,3] S. Murayama,[2] and A. Takashima[1]

[1]Laboratory for Alzheimer's Disease, RIKEN Brain Science Institute, Wako-shi, Saitama, Japan
[2]Department of Neuropathology, Tokyo Metropolitan Institute of Gerontology, Tokyo, Japan
[3]Department of Pathology, Tokyo Metropolitan Geriatric Hospital, Tokyo, Japan

Intracellular accumulation of filamentous tau proteins is a defining feature of neurodegenerative diseases termed *tauopathies*. The pathogenesis of tauopathies remains largely unknown. Molecular chaperones such as heat shock proteins (HSPs), however, have been implicated in tauopathies as well as in other neurodegenerative diseases characterized by the accumulation of insoluble protein aggregates. To search for in vivo evidence of chaperone-related tau protein metabolism, we analyzed human brains with varying degrees of neurofibrillary tangle (NFT) pathology, as defined by Braak NFT staging. Quantitative analysis of soluble protein levels revealed significant positive correlations between tau and Hsp90, Hsp40, Hsp27, α-crystallin, and CHIP. An inverse correlation was observed between the levels of HSPs in each specimen and the levels of granular tau oligomers, the latter of which were isolated from brain as intermediates of tau filaments. We speculate that HSPs function as regulators of soluble tau protein levels, and, once the capacity of this chaperone system is saturated, granular tau oligomers form virtually unabated. This is expressed pathologically as an early sign of NFT formation. The molecular basis of chaperone-mediated protection against neurodegeneration might lead to the development of therapeutics for tauopathies.

Key words: tau; oligomer; heat shock protein; molecular chaperone; Braak stage

Intracellular accumulation of filamentous tau proteins is a defining feature of neurodegenerative diseases, including Alzheimer's disease (AD), progressive supranuclear palsy, corticobasal degeneration, Pick's disease, and frontotemporal dementia with Parkinsonism linked to chromosome 17, all known collectively as *tauopathies* (Lee et al., 2001). Tau is a highly soluble and natively unfolded protein dominated by a random coil structure in solution (Schweers et al., 1995). It is believed that aberrant modifications of tau, including phosphorylation, truncation, and conformational changes, induce filamentous aggregation (Alonso et al., 1996; Gamblin et al., 2003; Garcia-Sierra et al., 2003). In AD and related tauopathies correlated with dementia, tau generates insoluble aggregates (Arriagada et al., 1992). Although the mechanism underlying the conversion of tau protein from a soluble state to one of insoluble aggregates remains unclear, molecular chaperones such as heat shock proteins (HSPs) have been implicated in these tauopathies (Dabir et al., 2004; Nemes et al., 2004).

Molecular chaperones have essential roles in many cellular processes, including protein folding, targeting, transport, degradation, and signal transduction (Hartl and Hayer-Hartl, 2002). In addition to molecular chaperones, cells have evolved two mechanisms for degrading misfolded proteins, the ubiquitin-proteasome pathway and lysosome-mediated autophagy. The collective activities of molecular chaperones, the ubiquitin-proteasome system, and lysosome-mediated autophagy are normally sufficient to prevent the accumulation of misfolded proteins. In AD, Parkinson's disease, familial amyotrophic lateral sclerosis, and polyglutamine diseases, plaques and/or inclusion bodies that characterize these diseases colocalize with various molecular chaperones (Muchowski and Wacker, 2005) and components of the ubiquitin-proteasome degradation system (Sherman and Goldberg, 2001).

Recently, the carboxyl terminus of Hsc70-interacting protein (CHIP) was demonstrated to regulate tau

Contract grant sponsor: RIKEN BSI; Contract grant sponsor: Grant-in-Aid for Science Research from the Japanese Ministry of Education, Science, Sports and Culture (to A.T.).

*Correspondence to: N. Sahara, Laboratory for Alzheimer's Disease, RIKEN Brain Science Institute, Wako-shi, Saitama 351-0198, Japan. E-mail: saharanaruhiko@brain.riken.jp

Received 28 February 2007; Revised 25 April 2007; Accepted 26 April 2007

Published online 12 July 2007 in Wiley InterScience (www.interscience.wiley.com). DOI: 10.1002/jnr.21417

ubiquitination and degradation (Hatakeyama et al., 2004; Petrucelli et al., 2004; Shimura et al., 2004b). CHIP is a key molecule in protein quality control processes that link the ubiquitin-proteasome and chaperone systems. We previously found increased levels of CHIP in AD brains that were inversely proportional to the amount of accumulated tau (Sahara et al., 2005). Deletion of CHIP in mice, however, failed to promote tau aggregation (Sahara et al., 2005; Dickey et al., 2006b). Thus, these observations could not clarify the precise roles of the chaperone and ubiquitin-proteasome systems in the pathogenesis of tauopathies. Immunohistochemical studies also showed that AD brains contain very few accumulations of CHIP within neurofibrillary tangle (NFT)-bearing neuron (Petrucelli et al., 2004). Indeed, the colocalization of tau pathology and chaperones varies, as demonstrated by immunostaining for tau, Hsp27, αB-crystallin (Dabir et al., 2004), Hsp70, and Hsp90 (Dou et al., 2003). These observations suggest that tau in a misfolded conformation or state, not tau in an irreversible filamentous state, may exist and be directly regulated as a chaperone client. For this reason, we continue to search for intermediate forms of tau fibrils by examining assembled recombinant tau and tau in human brain extracts. Atomic force microscopy (AFM) has revealed a granular-shaped prefilamentous form of tau in both in vitro and in vivo preparations (Maeda et al., 2006, 2007).

In the present study, human brains with varying degrees of Braak-staged NFT pathology were analyzed to assess tau protein quality control in vivo. Biochemically, HSPs and related proteins were quantitatively analyzed to examine the relationship between tau and HSPs. A positive correlation was revealed between tau and certain HSPs in terms of soluble protein levels. Moreover, we discovered an inverse correlation between the levels of granular tau oligomer and those of HSPs. These findings suggest that molecular chaperones interact with soluble tau protein to down-regulate the formation of granular tau oligomer.

MATERIALS AND METHODS

Post-Mortem Brains

Brain tissue was obtained from the Brain Bank for Aging Research at Tokyo Metropolitan Institute of Gerontology (TMIG) and Tokyo Metropolitan Geriatric Hospital (TMGH). Frontal and temporal cortices were examined from each brain specimen. Senile plaques and NFTs were classified based on quantitative pathological features according to Braak criteria (Braak and Braak, 1991). Demographic information for all brain specimens analyzed is presented in Table I and in a previous report (Maeda et al., 2006). This study was approved by the Institutional Review Board (IRB) of TMIG and TMGH as well as the RIKEN IRB.

Tissue Extraction

Frontal and temporal cortices from each subject were homogenized separately in three volumes of Tris-buffered saline (TBS) containing protease and phosphatase inhibitors [25 mM Tris/HCl, pH 7.4; 150 mM NaCl; 1 mM EDTA; 1 mM EGTA; 5 mM sodium pyrophosphate; 30 mM β-glycerophosphate; 30 mM sodium fluoride; and 1 mM phenylmethylsulfonyl fluoride (PMSF)]. The homogenates were centrifuged at 27,000*g* for 15 min at 4°C to obtain supernatant (TBS sup) and pellet fractions. Pellets were rehomogenized in three volumes of high-salt/sucrose buffer (0.8 M NaCl; 10% sucrose; 10 mM Tris/HCl, pH 7.4; 1 mM EGTA; 1 mM PMSF) and centrifuged as described above. The supernatants were collected and incubated with sarkosyl (Sigma, St. Louis, MO; 1% final concentration) for 1 hr at 37°C, followed by centrifugation at 150,000*g* for 1 hr at 4°C to obtain salt and sarkosyl-soluble and sarkosyl-insoluble pellets (srk-ppt fractions).

TABLE I. Demographic and Neuropathological Characteristics of Subjects*

Case no.	Age (years)	Sex	PMI (hr:min)	Braak stage[a] NFT	Braak stage[a] SP	Insoluble tau[b] Frontal	Insoluble tau[b] Temporal
1	52	M	15:51	0	0	0.86	0.70
2	69	F	11:48	0	A	0.45	1.06
3	82	F	39:04	0	0	2.34	1.23
4	87	M	70:10	0	0	0	1.86
5	78	M	2:02	0	0	0	9.73
6	66	F	9:51	0	B	0	2.44
7	81	M	3:00	I	B	1.00	10.82
8	97	F	2:40	I	B	7.00	3.34
9	84	M	47:25	I	B	0	4.48
10	87	M	4:25	I	C	1.94	19.1
11	93	M	20:49	I	C	3.38	69.5
12	86	F	6:50	III	C	1.93	100.4
13	94	M	13:00	III	C	2.56	73.3
14	87	F	4:21	III	C	6.81	209.5
15	82	F	10:32	III	C	31.1	184.8
16	89	F	16:11	III	C	7.03	88.6
17	90	F	64:07	V	C	182.5	2189.6
18	86	F	19:51	V	C	86.2	1026.5
19	93	F	13:28	V	C	169.8	1091.2
20	70	M	35:42	V	C	582.8	1580.1
21	80	F	6:41	V	C	9.60	223.4

*NFT, neurofibrillary tangle; SP, senile plaque; PMI, post-mortem interval.

[a]For the staging of NFTs and SPs, Braak and Braak criteria were applied (Braak and Braak, 1991).

[b]The relative score of sarkosyl-insoluble tau was measured by quantifying PHF1 immunoreactivity.

Western Blotting

Fractionated tissue extracts were dissolved in sample buffer containing β-mercaptoethanol (0.01%). The boiled extracts were separated by gel electrophoresis on 10% or 4–20% gradient SDS-PAGE gels and transferred onto nitrocellulose membranes (Schleicher & Schuell Bioscience, Dassel, Germany). After blocking with a solution of 5% nonfat milk and 0.1% Tween-20 in PBS, the membranes were incubated with various antibodies, washed to remove excess antibodies, and then incubated with peroxidase-conjugated goat anti-

rabbit IgG (1:5,000; Jackson Immunoresearch, West Grove, PA) or anti-mouse IgG (1:5,000; Jackson Immunoresearch). Bound antibodies were detected by using an enhanced chemiluminescence system, SuperSignal West Pico (Pierce Biotechnology, Rockford, IL). Quantitation and visual analysis of immunoreactivity were performed with a computer-linked LAS-3000 Bio-Imaging Analyzer System (Fujifilm, Tokyo, Japan) in the software Image Gauge 3.0 (Fujifilm).

Antibodies

Polyclonal antibody E1, which is specific for human tau (aa 19–33; Sahara et al., 2005), and polyclonal antibody tauC, which is specific for the C-terminus of tau (aa 422–438; Sato et al., 2002), were produced in our laboratory. Monoclonal antibody Tau5, which is against an epitope located within the middle region of tau, was purchased from Biosource International (Camarillo, CA). PHF1, which is specific for tau phosphorylated at Ser396/Ser404, was provided by Dr. Peter Davies (Jicha et al., 1999). Polyclonal CHIP antibodies (R1) were produced in rabbits (Imai et al., 2002). Monoclonal antibodies to Hsp90 (Santa Cruz Biotechnology, Santa Cruz, CA), Hsp70 (Chemicon, Temecula, CA), Hsp60 (Stressgen, San Diego, CA), Hsp27 (Stressgen), αB-crystallin (Stressgen), β-tubulin (Sigma), β-actin (Sigma), glyceraldehyde-3-phosphate dehydrogenase (GAPDH; Chemicon), and neuron-specific enolase (NSE; Upstate, Charlottesville, VA) were purchased. Polyclonal antibodies against Hsc70 and Hsp40 were purchased from MBL and Stressgen. For Western blotting, antibodies were used at the following dilutions in blocking solution: E1, 1:5,000; tau5, 1:2,000; tauC, 1:5,000; PHF1, 1:2,000; CHIP, 1:5,000; Hsp90, 1:2,000; Hsp70, 1:1,000; Hsc70, 1:1,000; Hsp60, 1:5,000; Hsp40, 1:10,000; Hsp27, 1:1,000; αB-crystallin, 1:1,000; Akt, 1:2,000; β-tubulin, 1:5,000; β-actin, 1:10,000; GAPDH, 1:5,000; NSE, 1:1,000.

Coimmunoprecipitation Analysis

TBS-soluble fractions were incubated with anti-tau antibody JM (an antibody against the longest isoform of recombinant human tau; Takashima et al., 1998) for 2 hr at 4°C. Protein G-sepharose (GE Healthcare Bioscience, Piscataway, NJ) equilibrated in TBS was added to the mixture, which was then rotated overnight at 4°C. The resin was separated by centrifugation, washed four times with TBS, and then boiled in SDS sample buffer. Samples were subjected to SDS-PAGE, with subsequent immunoblotting with antibodies against Hsp90, Hsp70, β-tubulin, tau (anti-tau antibody HT7; Innogenetics, Zwijndrecht, Belgium), and NSE.

Purification of Granular Tau Oligomers

Enriched granular tau oligomer preparations were prepared as previously described (Maeda et al., 2006, 2007). Briefly, soluble fractions of human brain extracts (starting wet weight was ~12 g) were loaded onto an immunoaffinity column containing anti-tau antibody-conjugated Sepharose. Eluted samples were further purified by sucrose-step gradient centrifugation. Granular tau oligomer-enriched fractions were morphologically characterized by AFM.

Atomic Force Microscopy

Samples were dropped onto freshly cleaved mica and left in place for 30 min prior to AFM assessment. After washing the mica with water, we examined the tau-containing samples in solution using a Nanoscope IIIa (Digital Instruments, Santa Barbara, CA) set to tapping mode. OMCL-TR400PSA (Olympus, Tokyo, Japan) was used as a cantilever. The resonant frequency was about 9 kHz. We examined four different areas (4 μm^2) of the mica surface covered with granular aggregates. These areas were analyzed with NIH Image 1.63 (developed at The National Institute of Mental Health and available on the Internet at http://rsb.info.nih.gov/nih-image/), and summations of four different areas were demonstrated.

Incubation of Recombinant Tau and Fluorescence Spectroscopy

Recombinant human tau (2N4R) was expressed in *Escherichia coli* BL21(DE3) and partially purified as described previously (Hasegawa et al., 1998). The degree of tau aggregation was determined using thioflavin T (ThT). The tau stock solution was diluted to 10 μM in a solution containing PBS (pH 7.4) and 10 μM ThT (Aldrich Chemical, Milwaukee, WI), then loaded into 96-well Black Cliniplates (Thermo Labsystems, Yokohama, Japan). Tau assembly was initiated by adding 10 μM heparin (Acros Organics, Geel, Belgium) and incubating mixtures (final volume of 50 μl per well) at 37°C. To analyze the effects of HSPs, 0.1 μM or 1 μM Hsp70 (Sigma) and 0.1 μM or 1 μM Hsp40 proteins (Stressgen) were added alone or in combination to the aggregation reaction in the presence of 1 mM ATP at time zero. Fluorescence was measured with an ARVO MX Multilabel counter (PerkinElmer, Waltham, MA) at an excitation wavelength of 440 nm and an emission wavelength of 486 nm. Measurements were carried out at the time points indicated.

Fig. 1. Immunoblotting of sarkosyl-insoluble and TBS-soluble tau in frontal and temporal cortices from aged human brains. **A:** Western blots of sarkosyl-insoluble fractions in human frontal and temporal cortices. Samples were categorized as Braak NFT stage 0 (lanes 1–6), stage I (lanes 7–11), stage III (lanes 12–16), and stage V (lanes 17–21). Samples derived from brains (2–20 mg wet weight) were separated by SDS-PAGE, blotted, then probed with PHF1 antibody. Blot of frontal cortical samples was obtained from longer exposure time than that of temporal cortical samples. **B:** Western blots of TBS-soluble tau in human frontal and temporal cortices. Equal volumes of TBS-soluble fraction derived from 0.33 mg wet weight of brain were separated by SDS-PAGE, blotted, then probed with E1 (specific for N-terminus region of tau), tau5 (specific for the middle region), and tauC (specific for C-terminus region) antibodies. **C:** Western blots of TBS-soluble tau in human frontal and temporal cortices. Equal volumes of TBS-soluble fraction were separated by SDS-PAGE, blotted, then probed with the indicated panel of antibodies.

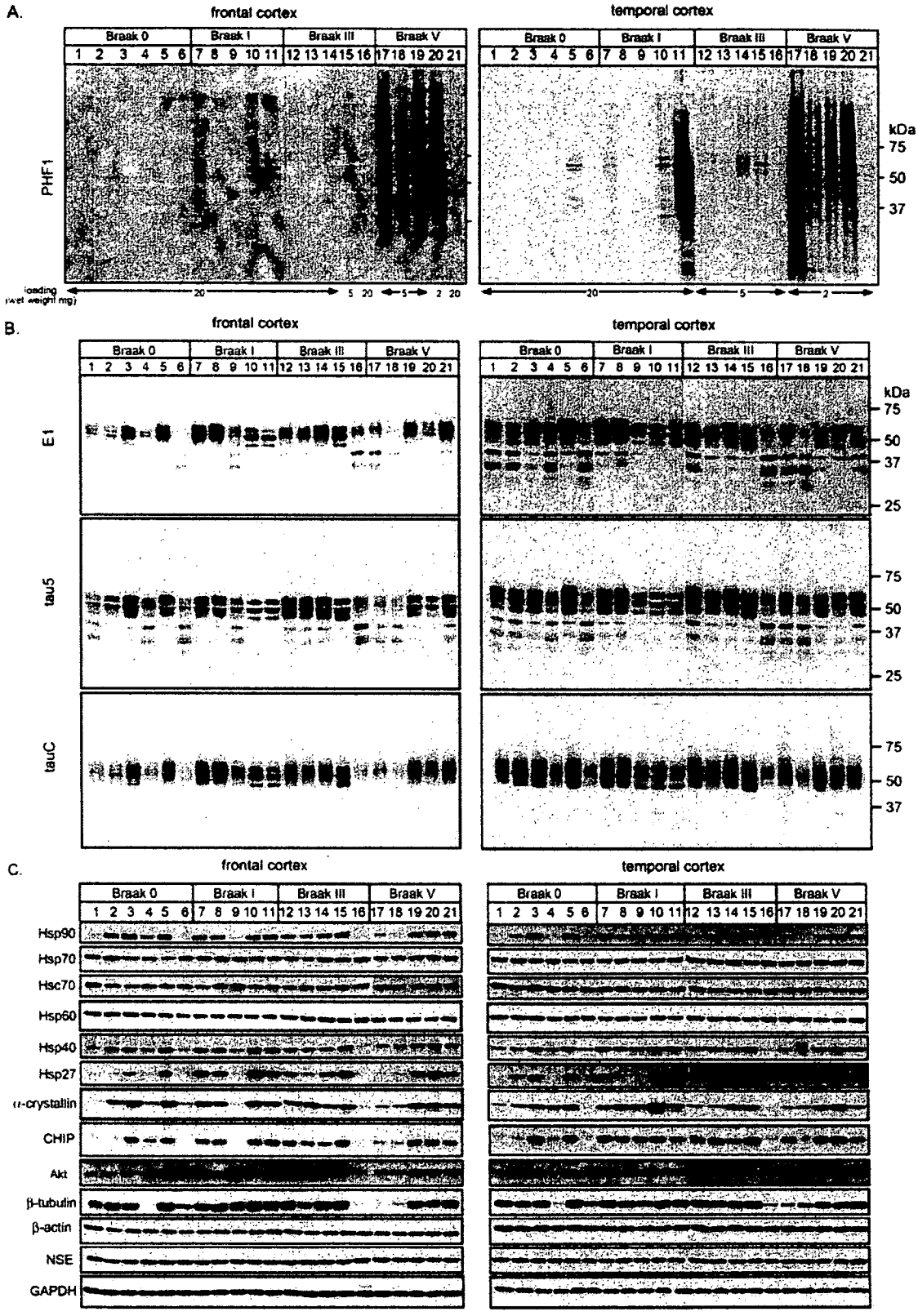
A.
frontal cortex
temporal cortex
Braak 0
Braak I
Braak III
Braak V
1 2 3 4 5 6 7 8 9 10 11 12 13 14 15 16 17 18 19 20 21
PHF1
kDa
75
50
37
loading (wet weight mg)
20
5 20
5
2 20
B.
frontal cortex
temporal cortex
E1
tau5
tauC
kDa
75
50
37
25
C.
frontal cortex
temporal cortex
Hsp90
Hsp70
Hsc70
Hsp60
Hsp40
Hsp27
α-crystallin
CHIP
Akt
β-tubulin
β-actin
NSE
GAPDH

Figure 1.

Statistical Analysis

The statistical significance between groups was assessed by the Mann-Whitney test. The correlation between the level of tau and other proteins was tested using Spearman correlation. Data were analyzed with Prism for Macintosh version 4.0b (Graphpad, San Diego, CA), and significance levels were set at $P < 0.05$.

RESULTS

Sarkosyl-Insoluble Tau in Human Brain

The neuropathological diagnoses of 21 cases were determined by using criteria for degenerative dementia as previously reported (Saito et al., 2002). To verify NFT pathology, we performed Western blotting on sarkosyl-insoluble fractions obtained from these 21 cases. The amounts of sarkosyl-insoluble tau in both frontal and temporal cortices correlated well with various Braak NFT stages (Fig. 1A, Table I). Immunoblots of fractions from Braak V-staged brains displayed the typical triplet bands and smear patterns of PHF1-positive tau. Although low sarkosyl-insoluble tau levels correlated well with Braak 0 and I stages—stages seen during normal brain aging characterized by the absence of NFT pathology in frontal and temporal cortices—weak PHF1-positive tau immunostaining was observed in one Braak 0 brain (case 5) and three Braak I brains (cases 7, 10, and 11; Fig. 1A, Table I). Indeed, some discrepancies have been reported regarding insoluble tau levels and NFT scores of brains staged at Braak stages I–III (Katsuno et al., 2005). Together, these results indicated that the biochemical analysis was more sensitive in detecting precursors of NFTs (i.e., PHF1-positive tau) than was the Braak neuropathological classification method. Nonetheless, for one Braak V brain (case 21), we detected very low levels of sarkosyl-insoluble tau. In case 21, these levels were equivalent to those detected in Braak III brains (Table I), suggesting that, despite reliable neuropathological diagnosis, an unknown tau modification might have occurred in this case. In any case, it is important to identify an early biochemical indicator of AD rather than to measure levels of sarkosyl-insoluble tau.

TBS-Soluble Tau Protein Profiles in Human Brains

As shown in Figure 1B, a wide range of TBS-soluble tau levels and variable Western blot profiles were observed among the human brains that we analyzed. Although we suspected that protein degraded during post-mortem intervals, the amounts of TBS-soluble tau in frontal and temporal cortices did not correlate with different postmortem intervals (Fig. 2A,B). For most of the samples, E1 and tau5 antibodies, which recognize the amino terminus and the middle regions of tau, respectively, immunostained low-molecular-weight bands ranging from 30 to 40 kDa (Fig. 1B). These bands, however, were not detectable with tauC antibody, which recognizes the carboxyl terminus of tau. This suggests that carboxyl-terminal-truncated tau fragments 30–40 kDa in size were present in these samples. For each case, the profile of tau protein in frontal cortex and that in temporal cortex appeared quite similar (Fig. 1B). Moreover, the relative levels of tau protein in frontal and temporal cortices were closely correlated ($P < 0.001$, Spearman correlation analysis). This result indicated that tau protein modification was conserved in different brain regions. Comparison of the amounts of TBS-soluble tau in brains of different Braak stages revealed significant differences in the frontal and temporal cortices of Braak I and V brains (Fig. 2G,H). These differences might be due to a conversion in tau protein solubility that results from excessive posttranslational modifications in Braak V brains, leading to the formation of filamentous insoluble tau. However, we did not observe a significant inverse correlation between TBS-soluble tau and sarkosyl-insoluble tau levels. Further study will be needed to clarify why Braak I and V brains contain different levels of soluble tau protein.

Correlation Between Tau Protein and HSPs

We used a panel of antibodies to identify HSPs (Hsp90, Hsp70, Hsc70, Hsp60, Hsp40, Hsp27, α-crystallin) and cochaperone CHIP in human frontal and temporal cortices (Fig. 1C). As with TBS-soluble tau levels, Hsp90 and NSE protein levels in frontal and temporal cortices did not correlate with different post-mortem intervals (Fig. 2C–F). Quantitative analysis of soluble protein levels in frontal cortices revealed significant positive correlations between tau and some HSPs (Hsp90, Hsp40, Hsp27, α-crystallin), CHIP, Akt, and β-tubulin (Table II). We obtained comparable results for soluble protein levels in temporal cortices (Fig. 1, Table II). Hsp90, Hsp40, Hsp27, α-crystallin, CHIP, Akt, and β-tubulin levels varied across different Braak stages, with

Fig. 2. Effect of post-mortem time and Braak NFT stage on relative protein levels. **A–F:** Relationship between postmortem interval (hours) and soluble protein levels. The relative amount of TBS-soluble tau in frontal (A) and temporal (B) cortices was calculated by dividing the intensity of tauC-immunoreactive bands by the intensity of GAPDH-positive bands. The relative amounts of Hsp90 in frontal (C) and temporal (D) cortices and NSE in frontal (E) and temporal (F) cortices were calculated by dividing the appropriate band intensity by the band intensity of GAPDH. The relative amount of protein in case 7 was always normalized to 1. **G,H:** The relative levels of TBS-soluble tau in frontal (G) and temporal (H) cortices were compared for each Braak NFT stage. The relative amounts of TBS-soluble tau, as shown in A and B, were categorized accordingly into Braak NFT stage 0, I, III, or V. The results are shown as scatterplots of mean values. $*P < 0.05$, $**P < 0.01$.

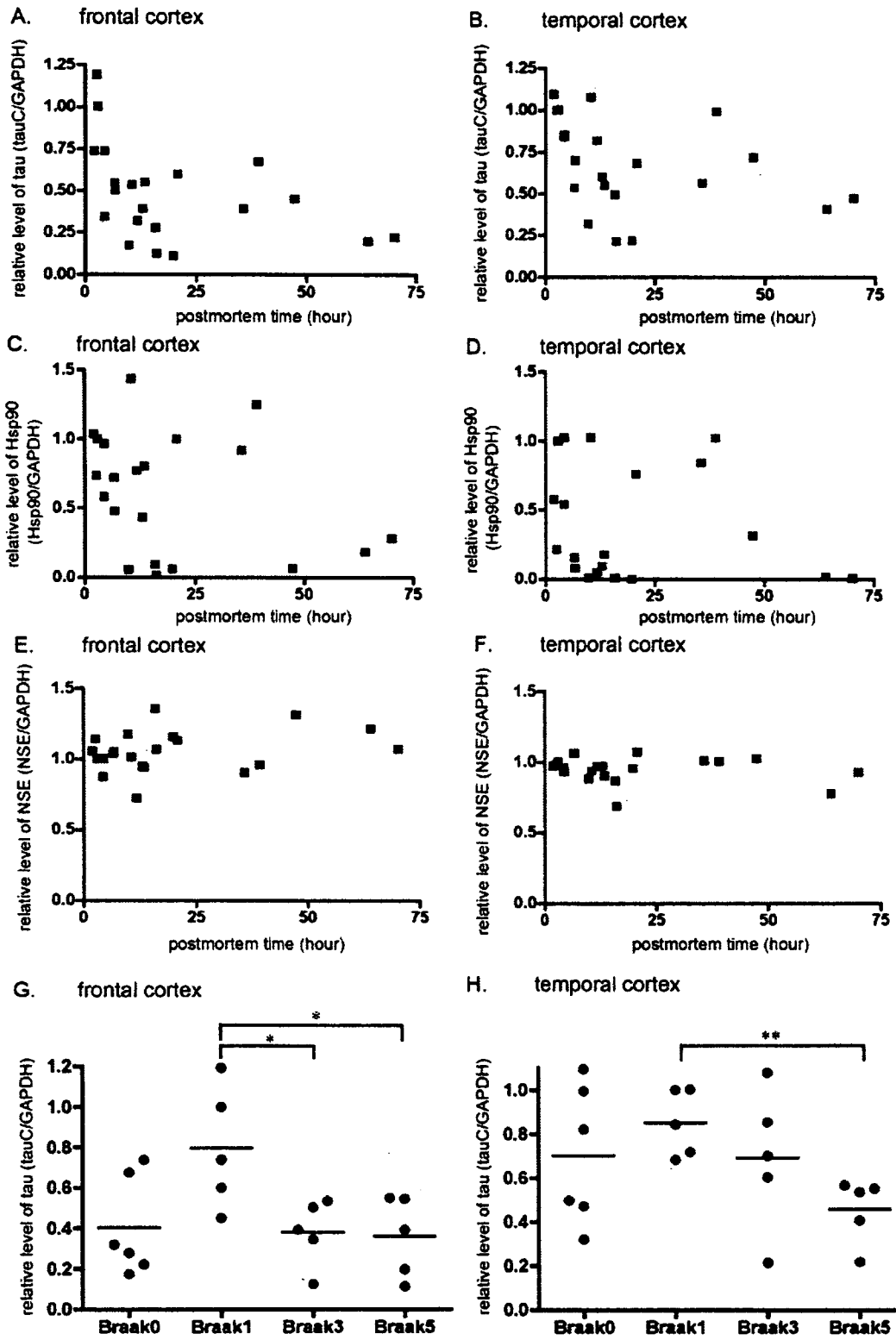
A.
frontal cortex
relative level of tau (tauC/GAPDH)
postmortem time (hour)
B.
temporal cortex
relative level of tau (tauC/GAPDH)
postmortem time (hour)
C.
frontal cortex
relative level of Hsp90 (Hsp90/GAPDH)
postmortem time (hour)
D.
temporal cortex
relative level of Hsp90 (Hsp90/GAPDH)
postmortem time (hour)
E.
frontal cortex
relative level of NSE (NSE/GAPDH)
postmortem time (hour)
F.
temporal cortex
relative level of NSE (NSE/GAPDH)
postmortem time (hour)
G.
frontal cortex
relative level of tau (tauC/GAPDH)
Braak0
Braak1
Braak3
Braak5
H.
temporal cortex
relative level of tau (tauC/GAPDH)
Braak0
Braak1
Braak3
Braak5

Figure 2.

TABLE II. Regional Correlation Analysis Between Tau and Other Proteins*

	Frontal cortex		Temporal cortex	
	Spearman regression	*P* value	Spearman regression	*P* value
Hsp90	0.789	<0.001	0.794	<0.001
Hsp70	−0.242	0.291	−0.186	0.420
Hsc70	−0.190	0.410	−0.143	0.537
Hsp60	0.085	0.714	−0.251	0.273
Hsp40	0.828	<0.001	0.723	<0.001
Hsp27	0.757	<0.001	0.562	0.008
α-Crystallin	0.801	<0.001	0.707	<0.001
CHIP	0.739	<0.001	0.751	<0.001
Akt	0.869	<0.001	0.768	<0.001
β-Tubulin	0.833	<0.001	0.779	<0.001
β-Actin	0.400	0.072	0.197	0.391
NSE	−0.283	0.214	0.449	0.041

*Soluble tau levels were obtained by dividing the intensity of tauC-immunopositive bands by the intensity of GAPDH-positive bands.

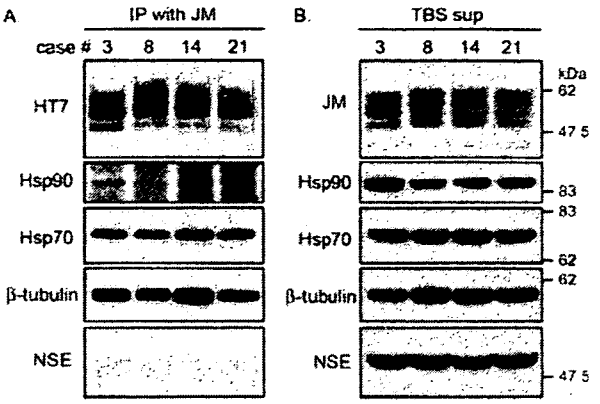

Fig. 3. Coimmunoprecipitation assay of human brain extracts. **A:** TBS-soluble fractions derived from temporal cortices (cases 3, 8, 14, and 21) were immunoprecipitated with anti-tau antibody JM. The resulting samples were immunoblotted with antibodies against HT7, Hsp90, Hsp70, β-tubulin, and NSE. **B:** TBS-soluble fractions were also subjected to SDS-PAGE and immunoblotted with the indicated antibodies.

samples from Braak I-staged brains tending to contain more of these proteins. In contrast, Hsp70, Hsc70, Hsp60, β-actin, NSE, and GAPDH levels remained steady across different Braak stages and within each cortical region. Quantitative analysis clearly showed that the levels of all soluble proteins did not correlate with the levels of sarkosyl-insoluble tau, more of which was recovered in temporal cortices than in frontal cortices. Moreover, we did not observe any significant correlation between HSP levels and senile-plaque stage (Table I). These data suggest that a molecular chaperone complex (Hsp90, Hsp40, Hsp27, α-crystallin, and CHIP) interacts with Akt, β-tubulin, and tau as client proteins in aged human brains and that this complex is elevated during the Braak I stage.

To determine whether tau and the chaperone proteins physiologically interact in human brain, we analyzed brain extracts using a coimmunoprecipitation assay. Regardless of Braak stage, tau coimmunoprecipitated with Hsp90, Hsp70, and β-tubulin but with not NSE (Fig. 3). Surprisingly, Hsp70 was more efficiently recovered by anti-tau immunoprecipitation than Hsp90. Although the direct interaction between tau and these HSPs remains to be demonstrated, these data support the hypothesis that tau and Hsp90/Hsp70 physiologically interact.

Correlation Between HSP Levels in Soluble Fraction and Granular Tau Oligomer

Previously, the identification of granular tau oligomers as intermediates of tau filaments from human frontal cortices was reported (Maeda et al., 2006). Granular tau oligomer levels in frontal cortex were increased even in brains displaying Braak I characteristics (Fig. 4A,B), suggesting that granular tau oligomers may form before NFTs form. To evaluate these oligomers further, we compared oligomer levels from each specimen to HSP levels and observed a significant inverse correlation between oligomer and Hsp90 levels (Fig. 4D; oligomers vs. Hsp90, $P = 0.045$) and between oligomer and α-crystallin levels (oligomers vs. α-crystallin, $P = 0.029$). When data from Braak 0 samples were excluded from the correlation analyses, we found that Hsp40, Hsp27, α-crystallin, CHIP, and Akt levels also showed a significant inverse correlation with oligomer levels (Hsp40 $P < 0.001$, Hsp27 $P < 0.001$, α-crystallin $P < 0.001$, CHIP $P = 0.0015$, Akt $P = 0.0033$). Because the levels of these HSPs positively correlate with the levels of TBS-soluble tau, we were able to determine the relationship between tau oligomers and TBS-soluble tau in Braak-staged aged brains. Indeed, oligomer levels inversely correlated with TBS-soluble tau levels (Fig. 4C; oligomers vs. tauC-positive tau, $P = 0.015$). These findings suggest that TBS-soluble tau is a target of the HSP-mediated refolding complex, whereas granular tau oligomers are counterparts of this complex.

HSPs Prevent In Vitro Tau Self-Aggregation

To study the biochemical interaction between tau protein and HSPs, we analyzed in vitro tau polymerization in the presence and absence of Hsp40 and/or Hsp70 by using a ThT-binding assay. The thioflavin assay is the most commonly used assay to assess real-time tau assembly, because ThT binds β-sheet structures. With increased binding, more intense fluorescent signals are emitted (Kuret et al., 2005). As we previously described (Maeda et al., 2007), tau self-assembly was induced by adding heparin, after which ThT fluorescence levels plateaued after 100 hr (Fig. 5A). Tau prepared in the absence of heparin displayed no measurable

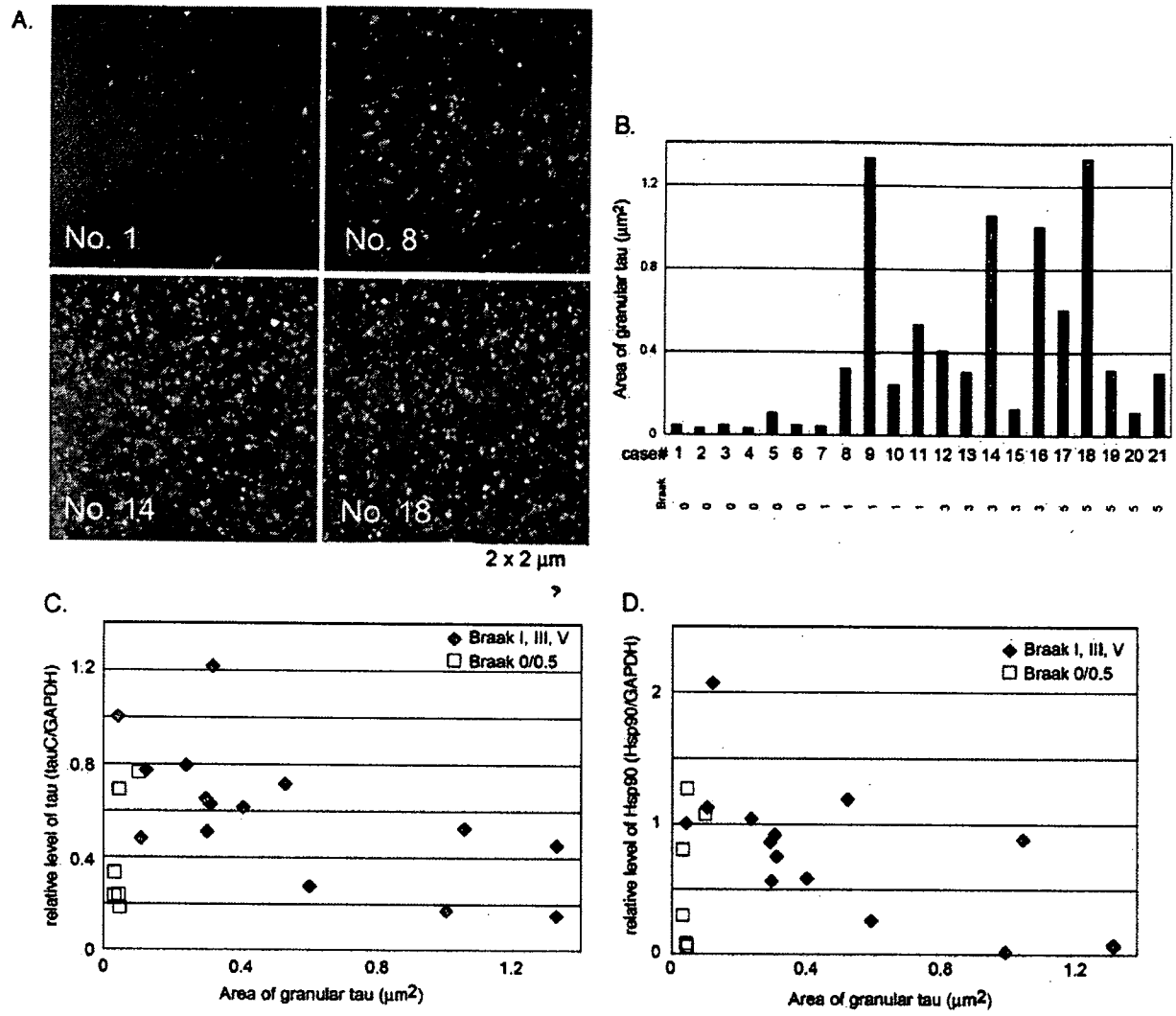

Fig. 4. Quantitative analysis of granular tau oligomer in human frontal cortices. **A:** AFM images of granular tau oligomers from representative Braak NFT-staged samples. Cases 1, 8, 14, and 18 were staged at Braak 0, I, III, and V, respectively. The size of each image size is 2 μm^2, and the height range is 30 nm. **B:** Quantitative data of granular tau oligomer is represented as the area (μm^2) occupied by tau granules. Each case and Braak NFT stage is indicated. **C,D:** Correlations between granular tau oligomer and tau levels (C) and oligomer and Hsp90 levels (D) are shown. Samples were grouped into Braak NFT stage 0 (squares) and Braak stages I, III, and V (diamonds).

fluorescent signals (data not shown). Because Hsp40 and Hsp70 form the initial recognition complex during the processing of client proteins of the chaperone network (Dickey et al., 2007), we added these HSPs to heparin-induced tau assembly preparations. Hsp40 and Hsp70 significantly reduced the ThT signals, but adding both Hsp40 and Hsp70 to the preparation reduced fluorescence even more, affecting tau assembly during the entire incubation period (Fig. 5). Interestingly, Hsp40 had a dose-dependent effect, whereas Hsp70 did not (Fig. 5B). These results indicate that Hsp40 and/or Hsp70 directly prevented the aggregation of tau protein. Further studies will be needed to clarify the refolding and degradation of tau protein related to molecular chaperones.

DISCUSSION

More than 20 neurodegenerative disorders are characterized by the presence of aggregates of the microtubule-binding protein tau (Lee et al., 2001). Tau protein forms insoluble NFTs that accompany and may promote neurodegeneration in these brain diseases. Details of the steps involved in the conversion of solu-